Ocean Sci. Discuss., 10, 1833–1893, 2013
www.ocean-sci-discuss.net/10/1833/2013/
doi:10.5194/osd-10-1833-2013

Ocean Science
Discussions
Open Access

Experiments with the Secchi disk

E. Aas[1], **J. Høkedal**[2], **and K. Sørensen**[3]

[1]Department of Geosciences, University of Oslo, Gaustadalleen 21, 0349 Oslo, Norway
[2]Narvik University College, Lodve Langesgt. 2, 8508 Narvik, Norway
[3]Norwegian Institute for Water Research, Gaustadalleen 21, 0349 Oslo, Norway

Received: 9 September 2013 – Accepted: 8 October 2013 – Published: 25 October 2013

Correspondence to: E. Aas (eyvind.aas@geo.uio.no)

Published by Copernicus Publications on behalf of the European Geosciences Union.

Abstract

The Secchi depth and its relationships to other properties of the sea water in the Oslofjord–Skagerrak area have been investigated. White and black disks of different sizes have been applied, and the Secchi depth has been observed with the naked eye, through colour filters and with a water telescope. Spectral luminances and illuminances have been calculated from recordings of radiance and irradiance. A theoretical expression for the Secchi depth has been tested against field observations, and statistical relationships between Secchi depths and attenuation coefficients have been determined. Effects of size, colour filters, sun glitter and ship shadow have been quantified. The possibility to estimate quanta irradiance, chlorophyll *a* and total suspended material has also been studied.

1 Introduction

1.1 Motivation for the present study

The threshold depth of observation for the Secchi disk is a direct measure of the vertical visibility in water, and it is one of several parameters used by environmental authorities to describe water quality. In some branches of aquatic science it is termed transparency. The depth is determined by the optical properties of the water and can therefore be related to these properties. The usefulness of such relationships is the main motivation for this study. Observations of the Secchi disk depth can never be satisfactory substitutes for direct recordings of the other optical properties, but they can serve as independent checks of these properties.

The Norwegian Institute for Water Research and the University of Oslo have collected numerous observations of the Secchi depth. We have analysed parts of this database to check some of the assumptions on which the Secchi depth theory is based, and to derive empirical relationships between the Secchi depth and other marine-

OSD
10, 1833–1893, 2013

optical properties. Different disks and a water telescope have been applied, and threshold depths have been determined by the naked eye as well as with coloured glass filters in front of the eye. The results are based on observations from the Oslofjord–Skagerrak area.

In Sect. 2 we present what is essentially Tyler's (1968) theory of the Secchi depth, and Sect. 3 describes the applied data sets and instruments and some of the regional characteristics of the marine light field. Section 4 estimates the different optical properties appearing in the theoretical expression for the Secchi depth, and the expression is compared to observations. In Sect. 5 an assumption about photopic vs. monochromatic attenuation coefficients is being tested, while empirical relationships between the Secchi depth and other optical properties are discussed in Sect. 6. The results are summed up in Sect. 7.

1.2 History

The visibility of the Pacific Ocean was studied by the Russian naval officer Otto von Kotzebue as early as 1817 by means of a red piece of cloth being lowered into the sea, and on one occasion by a white plate, according to Krümmel (1886). This is probably the first known scientific investigation of the optical properties of the ocean. Other early transparency measurements and occasional observations are mentioned by Boguslawski (1884), a later work by Krümmel (1907), and by Wernand (2010).

In 1866, almost fifty years after von Kotzebue's measurements, Alessandro Cialdi, Commander of the Papal Navy, published a report containing a section by Frater Pietro Angelo Secchi, where the factors influencing the visibility in the sea of submerged disks of different sizes and colourings were discussed (Secchi, 1866). In the years to come the white version of this device became a standard instrument in marine investigations. The disk is in some scientific communities referred to as "the white disk", and in others as "the Secchi disk", although the suggestion of using a white disk came from Cialdi.

Today the marine standard method of measurement is to lower a white disk, with a diameter of approximately 30 cm, supported on a cord and with its plane horizontal,

OSD
10, 1833–1893, 2013

from the ship rail and into the sea to a depth where the disk cannot any longer be seen. The disk is then hauled upwards to a depth where it once again can be recognized. The mean value of the two threshold depths is termed “the Secchi depth”. In limnology some communities prefer using a 20 cm disk, painted in black and white quarters, but this device will not be discussed in this paper.

However, during the first century of Secchi depth measurements a satisfactory theory describing the relationship between the threshold depth and the optical properties of the sea was missing. The factors influencing the depth were known (Krümmel, 1889), and Sauberer and Ruttner (1941) had set up the equations governing the contrast and the upward directed light, but the final step connecting the Secchi depth and the attenuation coefficients was not taken. According to Shifrin (1988) Gershun had solved the problem in 1940, but his results were published in Russian and therefore not well known outside the Soviet Union. In the western world the breakthrough came when Tyler (1968) applied a contrast formula, presented sixteen years earlier by Duntley (1952), to derive an expression for the Secchi depth. Holmes (1970) tested the constant of this expression by field measurements. A different contrast formula, including the halo of scattered light around the disk, was suggested by Levin (1980). Preisendorfer (1986) discussed the assumptions and limitations of the Secchi depth theory and procedure, using attenuation coefficients of photopic quantities.

Krümmel (1889) referred to observations made by Austrian oceanographers in the Adriatic and Ionian Seas in 1880 with disks of different metals and paintings. Lisitzin (1938) observed the Secchi disk through coloured glass filters in the Baltic Sea as early as in the 1920ies, and Takenouti (1950) did similar measurements in Japanese lakes. Højerslev (1977, 1978) succeeded in relating such glass filter observations to other marine-optical properties. Levin (1980) mentioned recordings with glass filters in the Black Sea. An interesting study of the black disk was made in 1988 by Davies-Colley. Haltrin (1998) reported observations with disks that were painted blue, green and red.

OSD
10, 1833–1893, 2013

For more than two decades remote sensing of water colour has been used to estimate the Secchi depth, which is one of the ESA GlobColour products (http://www.globcolour.info/data_access_demo.html).

2 Theory of the Secchi depth

Studies in air (Blackwell, 1946) have demonstrated that the human eye is able to distinguish a target from its background down to a lower limit or threshold value of the contrast between the target and its background. In our case the target is the Secchi disk, and the definition of the contrast C becomes $C = (L_D - L)/L$, where L_D is the luminance from the disk and L the luminance from the background. The eye integrates the total spectrum of radiances within the direction to the disk and the background, and weights these radiances by the eye's spectral sensitivity. The resulting integrals become the luminances L_D and L. If the eye of the observer is at the depth $z = 0$, which in this paper will mean just beneath the surface, or if a water telescope is being used, that is a tube through the water surface with a glass window at the bottom, then the observed contrast $C(0)$ at this depth between the nadir luminances $L_D(0)$ and $L(0)$ from the white Secchi disk and the background, respectively, will be

$$C(0) = \frac{L_D(0) - L(0)}{L(0)} \quad (1)$$

When the Secchi disk is lowered, $L(0)$ remains constant while $L_D(0)$ is reduced until the disk reaches the depth where it disappears from sight, namely the Secchi depth. Then $C(0)$ has been reduced to the threshold value C_t.

The photometric luminance is not a practical quantity if we want to use the *Equation of Radiative Energy Transfer*, because the luminance represents a spectral integral, and therefore its attenuation coefficients are not constant in space, even in optically homogeneous waters. However, when we determine the Secchi depth, we notice that

OSD
10, 1833–1893, 2013

the colour of the disk is the same as that of the surrounding waters. This colour corresponds to the wavelength region where the water has its maximum beam transmittance, which is also where the upward scattered radiance obtains its spectral maximum. We can therefore assume as a first approximation that the observed luminances in Eq. (1) correspond to the radiances at the wavelength of the spectral transmittance maximum. In the present discussion we have let the symbol L represent these radiances as well as the spectrally narrow-banded luminances. The magnitude of the errors introduced by the monochromatic assumption will be discussed in Sect. 5.

The *Equation of Radiative Energy Transfer* for the nadir radiance L_D from the Secchi disk sounds

$$-\frac{dL_D(z)}{dz} \approx -cL_D(z) + L_{*D}(z) \quad (2)$$

where z is the vertical coordinate with zero at the surface and positive downwards, c is the beam attenuation coefficient at the wavelength of maximum transmittance, and L_{*D} is the path function along the path from the disk to the observer.

The same equation for the nadir radiance L from the background becomes

$$-\frac{dL(z)}{dz} \approx -cL(z) + L_*(z) \quad (3)$$

Here L_* is the path function along an upward directed path outside the disk.

Tyler (1968) applied Duntley's (1952) contrast formula and assumed that at each depth z the path function $L_{*D}(z)$ above the Secchi disk is practically uninfluenced by the disk, and therefore approximately equal to the path function $L_*(z)$ of the background. This assumption may be questioned, and especially at positions close to the disk. However, let us assume that it is still valid for most of the path between the disk and the surface. By making the approximation $L_{*D}(z) \approx L_*(z)$ and subtracting Eq. (3) from Eq. (2) we obtain

$$\frac{d[L_D(z) - L(z)]}{dz} \approx c[L_D(z) - L(z)] \quad (4)$$

OSD
10, 1833–1893, 2013

Provided c is constant with depth, the integration of this equation between the surface and the Secchi depth $z = Z_D$ results in

$$[L_D(0) - L(0)] = [L_D(Z_D) - L(Z_D)]e^{-cZ_D}. \quad (5)$$

We recognize the left side of this equation as the numerator of Eq. (1). On the right hand side we have the radiance $L_D(Z_D)$ which is the reflected part of the downward irradiance $E_d(Z_D)$ incident at the disk. The reflectance of this radiance may be termed ρ_{DL}, defined by

$$\rho_{DL} = \frac{L_D(Z_D)}{E_d(Z_D)} \quad (6)$$

At the same level outside the disk the upward radiance $L(Z_D)$ will be related to the downward irradiance by the radiance reflectance R_L:

$$R_L(Z_D) = \frac{L(Z_D)}{E_d(Z_D)}, \quad (7)$$

In Eqs. (6) and (7) it is assumed that the downward irradiance at the Secchi depth is practically unaffected by the presence of the disk, and has the same value above as outside the disk. By using Eqs. (6) and (7) the radiances on the right side of Eq. (5) may be written as functions of $E_d(Z_D)$, and Eq. (5) becomes

$$[L_D(0) - L(0)] = [\rho_{DL}E_d(Z_D) - R_L(Z_D)E_d(Z_D)]e^{-cZ_D} \quad (8)$$

At this point we see that it would be very convenient if we could also express the denominator $L(0)$ at the right hand side of Eq. (1) as a function of $E_d(Z_D)$. $L(0)$ can be transformed in several ways, but the simplest expression is obtained by using $E_d(z)$ and $R_L(z)$ and writing $L(z)$ as an exponential function of z:

$$L(0) = L(Z_D)e^{K_L Z_D} = R_L(Z_D)E_d(Z_D)e^{K_L Z_D} \quad (9)$$

OSD
10, 1833–1893, 2013

where K_L is the average vertical attenuation coefficients of $L(z)$ in the depth range 0–Z_D.

If we insert for the numerator in Eq. (1) from Eq. (8) and for the denominator from Eq. (9), we obtain:

$$C(0) = \frac{L_D(0) - L(0)}{L(0)} = \frac{[\rho_{DL} - R_L(Z_D)]e^{-cZ_D}}{R_L(Z_D)e^{K_L Z_D}} = \frac{[\rho_{DL} - R_L(Z_D)]}{R_L(Z_D)} e^{-(c+K_L)Z_D}, \quad (10)$$

which can be more conveniently written as

$$Z_D(c + K_L) = \ln\left(\frac{\frac{\rho_{DL}}{R_L(Z_D)} - 1}{C(0)}\right). \quad (11)$$

The contrast $C(0)$ is equal to the threshold value C_t, provided the eye of the observer is below the surface. Tyler (1968) presented a version of Eq. (11), and Hou et al. (2007) obtained a similar expression by using modulation transfer theory.

If the observer's eye is above the surface, the radiance from the direction of the disk will consist of two terms. The first is $L_D(0)\tau/n^2$, where τ is the radiance transmittance for a ray of normal incidence at the water–air interface, and n is the index of refraction for water. This is the transmitted part of the radiance $L_D(0)$. The other term is the radiance L_r from sun and sky reflected at the surface towards the observer. The sum of the terms becomes $L_D(0)\tau/n^2 + L_r$. Similarly the radiance from the background will now be $L(0)\tau/n^2 + L_r$. It should be noted that the first part of the latter sum is the quantity that is usually termed the water-leaving radiance L_w

$$L_w = L(0)\frac{\tau}{n^2}. \quad (12)$$

OSD
10, 1833–1893, 2013

The contrast of the Secchi disk observed in air through a flat sea surface becomes

$$C_{\text{air}} = \frac{\left(L_{\text{D}}(0)\frac{\tau}{n^2} + L_{\text{r}}\right) - \left(L(0)\frac{\tau}{n^2} + L_{\text{r}}\right)}{\left(L(0)\frac{\tau}{n^2} + L_{\text{r}}\right)} = \frac{L_{\text{D}}(0) - L(0)}{L(0)\left(1 + \frac{L_{\text{r}}}{L_{\text{w}}}\right)} = \frac{C(0)}{1 + \frac{L_{\text{r}}}{L_{\text{w}}}} \tag{13}$$

If capillary waves are present, they will have a blurring effect on the image of the disk, and as a result the apparent contrast will be reduced. Preisendorfer (1986) expressed the transmittance W of $C(0)$ at the water–air interface as a function of the angular subtense of the Secchi disk as seen from just below the surface, and the variance of the slopes of the capillary waves. In our notation his expression can be written

$$W = 1 - \exp\left(-\frac{D^2 k}{Z_{\text{D}}^2 U}\right) \leq 1, \tag{14}$$

where the symbols k and U represent the constant $787\,\text{m}\,\text{s}^{-1}$ and the wind speed, respectively, and D is the diameter of the disk. When W is included in Eq. (13), the equation becomes

$$C_{\text{air}} = \frac{C(0)}{1 + \frac{L_{\text{r}}}{L_{\text{w}}}} W = C_{\text{t}} \tag{15}$$

In this case it is C_{air} that represents the threshold value C_{t}. Equation (15) can also be written

$$C(0) = \frac{C_{\text{t}}}{W}\left(1 + \frac{L_{\text{r}}}{L_{\text{w}}}\right) \tag{16}$$

The contrast $C(0)$ has to be greater than C_{t}, and in inverse proportion to the blurring effect W. $C(0)$ will also be a linear function of the ratio $L_{\text{r}}/L_{\text{w}}$ between the reflected and

OSD
10, 1833–1893, 2013

water-leaving radiances. The greater the surface reflection is, the greater $C(0)$ has to be. It will be convenient for our purposes to express L_r and L_w as functions of the same input above the surface, namely the downward irradiance E_{air}. L_r can be written

$$L_r = \overline{\rho}_{L,air} E_{air} \tag{17}$$

where $\overline{\rho}_{L,air} = L_r/E_{air}$ is the Fresnel-reflected radiance towards the zenith, depending on the slope distribution of the surface and the angular distribution of radiance from sky and sun. L_w can be transformed by using the quantity $\Re$ introduced by Morel and Gentili (1996)

$$\Re = \frac{L_w}{L(0)} \frac{E_d(0)}{E_{air}} = \frac{L_w}{E_{air}} \frac{1}{R_L(0)} \tag{18}$$

By inserting for L_r and L_w from Eqs. (17) and (18) into Eq. (16) we obtain

$$C(0) = \frac{C_t}{W}\left(1 + \frac{L_r}{L_w}\right) = \frac{C_t}{W}\left(1 + \frac{\overline{\rho}_{L,air}}{\Re R_L(0)}\right) \tag{19}$$

Equation (11) can then be written, by substituting for $C(0)$ from Eq. (19),

$$Z_D(c + K_L) = \ln\left(\frac{\frac{\rho_{DL}}{R_L(Z_D)} - 1}{1 + \frac{\overline{\rho}_{L,air}}{\Re R_L(0)}} \frac{W}{C_t}\right) = \ln(A) \tag{20}$$

where A is defined as the product of the two fractions inside the greater parentheses. This is our basic equation for the threshold depth of the white Secchi disk observed from above the surface. The numerator of the first fraction is a function of the reflective properties ρ_{DL} of the disk and the radiance reflectance $R_L(Z_D)$ of the background at the Secchi depth, the denominator is a function of the ratio between the surface-reflected and water-leaving radiances, W represents the influence of capillary waves on the

OSD
10, 1833–1893, 2013

transmittance of $C(0)$ through the surface, while C_t is the threshold contrast of the human eye.

Observation of the disk through coloured glass filters will change the thresholds depths, and the coefficients c, K_L, ρ_{DL}, R_L, $\overline{\rho}_{L,air}$ and $\Re$ will refer to other wavelengths than the spectral region of maximum transmittance. Otherwise Eq. (20) remains the same.

Equation (20) contains 10 variables, and if we had precise values of these at a large number of stations, it would have been very interesting to test the equation. However, the usefulness of an expression needing the input of 9 variables to predict the one remaining would be limited. It would have been far more convenient if the right hand side of Eq. (20) had been a constant. The Secchi depth Z_D would then become linearly proportional to $1/(c+K_L)$, or $(c+K_L)$ would be proportional to $1/Z_D$. Unfortunately R_L, $\overline{\rho}_{L,air}$ and $\Re$ are variables determined by the optical properties of the sea water and sea surface, C_t is a function of the Secchi depth and the background luminance, while W varies with the wind speed and the Secchi depth. Thus the variables on the right hand side of Eq. (20) are neither independent nor constant, but the logarithmic function will reduce the variation of the expression inside the parentheses, which is why the equation still may provide a useful support for other marine-optical observations.

A more practical form of Eq. (20) for our purposes is

$$Z_D(c+K_L) = \ln\left(\frac{\rho_{DL}}{R_L(Z_D)} - 1\right) - \ln\left(1 + \frac{\overline{\rho}_{L,air}}{\Re R_L(0)}\right) + \ln(W) - \ln(C_t)$$
$$= \ln(A_1) - \ln(A_2) + \ln(W) - \ln(C_t) = \ln(A) \quad (21)$$

where A_1 and A_2 are defined by the expressions inside the parentheses. In order to test Eq. (21) we will calculate the mean value of the expression on the left hand side of the equation, as well as the mean values of the different logarithmic functions on the right hand side.

Some special cases can be pointed out:

OSD
10, 1833–1893, 2013

- For a perfectly black disk, that is a disk where $\rho_{DL} = 0$ (Eq. 6), the quantity A_1 of Eq. (21) obtains the value −1, while C_t will be a negative number. The two negative signs will cancel each other inside the parenthesis of ln(A).
- If $L_r/L_w \approx 0$ (Eq. 16 and 17), the quantity A_2 becomes 1 and ln(A_2) = 0.
- When Z_D is observed by using a water telescope, the effects of waves and surface-reflected sky radiance are eliminated, so that $W = 1$ in addition to $\overline{\rho}_{L,air} \approx 0$, and ln($A_2$) = ln($W$) = 0.

We will determine the attenuation coefficients c and K_L from calculated luminances in Sect. 4.1, estimate mean values of the different quantities on the right hand side of Eq. (21) in Sects. 4.2 and 4.3, and then see how the left hand side of the equation relates to this in Sect. 4.4. In Sects. 4.5–4.7 we will look at the effects of colour filters, disk size, sun glitter, ship shadow and waves.

3 Data sets, instruments and environmental conditions

Our main area of investigation has been the Oslofjord, with additional data from the Skagerrak (Fig. 1). The waters are in general eutrophic due to a supply of nutrients from the surrounding settlements. There is an estuarine circulation in the fjord, but rather weak in the inner part of the fjord. There will be an upper and a lower layer separated by a transition layer; the pycnocline. The surface layer may sometimes be well-mixed, but usually there is a gradual change of properties from the upper 1–2 m down to the pycnocline. The Secchi depth is found within the surface layer. Salinities in this layer are typically in the range 20–29, and in the deep waters up to 34. The Skagerrak serves as a transition zone between the North Sea and the Baltic (Aarup et al., 1996a, b; Højerslev et al., 1996), and it also supplies the more saline waters to the Oslofjord. A very thorough analysis of the Secchi depths in the North Sea–Baltic Sea region has been made by Aarup (2002). Surface salinities in the north-eastern

OSD
10, 1833–1893, 2013

part of the Skagerrak are in the range 25–32, and below the surface layer the waters become more Atlantic with salinities up to 35. Our observations of the Secchi depth with a standard disk are typically in the range 2–13 m, with a mean value of 6 m. The depth varies with location and time and is greater in winter than in summer. In our data sets the ranges of salinity S and Secchi depth Z_D are like this:

- Inner Fjord (north of 59.67° N): S = 15–28, Z_D < 14 m, N = 168
- Outer Fjord (59.00–59.67° N): S = 16–30, Z_D < 11 m, N = 48
- Skagerrak (57.00–59.00° N): S = 20–32, Z_D < 13 m, N = 32

N is the number of observations. Winter observations were restricted to the Inner Fjord, which is why the Secchi depth in this part obtains a greater value than in the other parts. Examples of Secchi depth maps for the Oslofjord have been presented elsewhere (Aas et al., 1989, the data were not included in the sets studied here). The accuracy of the Secchi depth measurement depends mainly on the state of the sea, and in our data the possible error will be in the range 0.2–0.5 m.

The first data set, collected in 1992 between 5 May and 8 December, contains the threshold depths of different types of Secchi disks observed in the Inner Oslofjord. The depths were observed above the surface of the sea by the open eye as well as with coloured glass filters. Measurements were also taken with a 3.0 m long water telescope (donated by N. K. Højerslev in Copenhagen) that reached from the ship rail into the sea. Two sizes of white and black disks were used, the standard size with a diameter of 30 cm, and a smaller one with a diameter of 10 cm. It is difficult to obtain a perfectly black disk, that is a disk with no reflectance at all. Disks painted black or made from black materials may still have a radiance reflectance ρ_{DL} that is greater than the corresponding reflectance R_L of the background water. The closest approximation to the non-reflecting disk that we have used has been a bowl-shaped lamp shade of brass, painted black for the scientific purpose, with diameter 30 cm. This device was originally acquired by the University of Copenhagen, but later on kindly donated to

OSD
10, 1833–1893, 2013

the University of Oslo. The instrument is supposed to work in principle very much like the light trap termed Rayleigh's Horn. The coefficients c and K_L were not recorded in 1992. The observations in this and the other data sets were all made by experienced oceanographers.

The second data set consists of Secchi depths, spectral irradiances, radiances, and absorption and attenuation coefficients at stations in the Oslofjord–Skagerrak area during the years 2002–2003, in the period from early May to early September. Vertical subsurface profiles of the downward and upward irradiances and the upward radiance were measured with the PRR-600 from Biospherical Instruments, San Diego, California, with the deck instrument PRR-610 used as a reference. The spectral channels were 412, 443, 490, 510, 555 and 665 nm, corresponding to the channels of the satellite sensors SeaWiFS and MERIS. Vertical profiles of the upward radiance L and the downward and upward irradiances E_d and E_u were recorded. According to the radiance model of Aas and Højerslev (1999), the quantity $Q = L/E_u$ should obtain values in the interval from π to 2π only, and a few stations where Q was lying outside this range have been omitted. Immersion coefficients determined by the manufacturer and self-shading effects (Gordon and Ding, 1992; Zibordi and Ferrari, 1995; Aas and Korsbø, 1997) were taken into account. Radiances and irradiances were plotted in semi-logarithmic diagrams and extrapolated up to the surface. The uncertainty of the resulting surface values was estimated to be ±10 %. A few series of spectral upward radiance just beneath the surface, recorded with the hyperspectral Ramses-ARC radiance sensor from TriOS, have been included to examine the wavelength of the spectral peak. Vertical profiles of the spectral absorption and scattering coefficients were recorded with an ac-9 from WET Labs, Philomath, Oregon. The applied instrument records at 412, 440, 488, 510, 532, 555, 650, 676, and 715 nm. The data were cleaned for obvious noise, and unrealistic spikes were avoided by using a median filter, resulting in an estimated uncertainty of ±10 %. The recordings with the Biospherical instrument and the ac-9 were analyzed and sent to the ESA for calibration and validation purposes (Sørensen et al., 2003, 2004, 2007). At 19 stations from the 2002–2003 data set chlorophyll *a* (Chl) and total suspended

OSD
10, 1833–1893, 2013

material (TSM) were sampled on glass fibre filters. The concentrations of Chl were determined by the high-performance liquid chromatographic (HPLC) method, and the TSM by a gravimetric method (Sørensen et al., 2007 and references therein).

A third data set consists of 143 stations from the Inner and Outer Oslofjord, collected between 1973 and 2008 by the University of Oslo during courses and project excursions, with recordings of quanta irradiance and Secchi depths. The period of observation included all months from February to December. Figure 1 shows the observation points for the three data sets.

The peak values of the upward spectral radiance spectra just beneath the surface usually occurred in a wavelength range from 480 to 570 nm, with the mean wavelength around 525 nm. The bluish maxima were only observed at stations that were strongly influenced by Atlantic waters (salinity close to 35). The half-peak bandwidths of the radiance spectra were typically 150 nm. When the radiance spectra are multiplied by the CIE 1924 photopic efficiency function (e.g. Walsh, 1958) in order to obtain the spectral upward luminances, the shapes of the spectra are significantly narrowed. The half-peak bandwidths will now be typically around 80 nm, and the peak values will lay between 550 and 570 nm. Table 1a presents statistical properties of the recorded spectral upward radiances and luminances, while Table 1b shows the results when the spectra have been normalized to the value at 555 nm. Table 1a is useful because it shows the absolute values of the upward spectra, while Table 1b makes it easier to evaluate the actual shapes of the spectra.

The properties of the photopic sensitivity of the eye alone and in combination with blue, green and red glass filters are shown in Table 2. The filters were produced by Schott and termed BG12, VG9 and RG1. The latter filter corresponds to OG590 in the latest Schott catalogue. The combined effect of eye sensitivity, filter transmittance and a typical spectrum of upward luminances $L(0)$ is also shown, and we see that the half-peak bandwidth of the naked eyed is reduced from 100 to 78 nm, otherwise the bandwidths and peak wavelengths remain the same.

OSD
10, 1833–1893, 2013

Average values for the inherent optical properties of the Skagerrak–Outer Oslofjord area were found by Sørensen et al. (2007). At 442 nm the absorption coefficient of yellow substance was $a_y(442) = 0.62\,\mathrm{m}^{-1}$, the bleached particle absorption $a_{bp}(442) = 0.065\,\mathrm{m}^{-1}$, and the particle scattering $b_p(442) = 0.645\,\mathrm{m}^{-1}$. The approximate spectral variations of these coefficients within the range 400–550 nm were $a_y(\lambda) = a_y(442)\,e^{-(0.0105\,\mathrm{nm}^{-1})(\lambda - 442\,\mathrm{nm})}$, $a_{bp}(\lambda) = a_{bp}(442)\,e^{-(0.0089\,\mathrm{nm}^{-1})(\lambda - 442\,\mathrm{nm})}$ and $b_p(\lambda) = b_p(442)\left[\frac{442\,\mathrm{nm}}{\lambda}\right]^{0.376}$ where λ is the wavelength, implying that the contributions from yellow substance and particles to the attenuation coefficient c are of the same order of magnitude in the blue part of the spectrum, while particles will tend to dominate in the red part.

4 Test of Eq. (21) in photopic units

4.1 Values of c_{phot} and $K_{L,\,phot}$

In Sect. 2 it was pointed out that the luminance is not a practical quantity in our marine-optical research, because the corresponding coefficient of beam attenuation will depend on the spectral shape of the luminance at the point where the attenuation starts and the distance along the beam. The coefficient c of Eq. (4) describes the beam attenuation of two different luminances: the upward luminance from the disk and the corresponding upward luminance from the surrounding waters. The radiance reflectance ρ_{DL} of the white Secchi disk is defined by Eq. (6). If the albedo of the disk had been 1 and the disk had acted like a perfect Lambert diffuser, the reflected radiance would have been constant for all directions with a radiance reflectance equal to $1/\pi = 0.32$. A real non-perfect Secchi disk will not have this value, but a number of the same order of magnitude. Tyler (1968) applied an estimate of ρ_{DL} equal to $0.82/\pi = 0.26$. Haltrin (1998) presented albedos for white and coloured disks, and provided the disks had acted like perfect diffusers, the values of ρ_{DL} for the white disk would have been 0.23–

OSD
10, 1833–1893, 2013

0.26–0.26 at 450–520–550 nm. In our laboratory the spectral downward irradiance E_d and the corresponding reflected upward radiance L_D from the white disk were measured in water just above the submerged disk. In order to avoid the shadow of the radiance meter on the disk, the instrument could not be held directly above it, but at an angle of 30–40° away from the axis of the disk. Still we think that the obtained values of ρ_{DL} were close to the correct ones, being 0.25–0.29–0.30 at the wavelengths 450–520–550 nm, respectively.

From the recorded spectral downward irradiances $E_d(Z_D)$ at the Secchi depth in the Oslofjord and Skagerrak the reflected upward radiances $L_D(Z_D)$ from the disk were then estimated by Eq. (6). The beam attenuations of the spectral radiances from this depth and up to the surface were calculated by applying recorded values of spectral c, and the resulting spectrum of radiances just beneath the surface was determined. The radiance spectra at the Secchi depth and at the surface were then integrated spectrally by using the photopic efficiency function, and from the resulting two luminances the efficient attenuation coefficient $c_{\text{phot, disk}}$ could be obtained. The attenuation coefficient c_{phot} of the upward background luminance $L(z)$ between the Secchi depth and the surface was calculated in a similar way. All values of the ratio $c_{\text{phot, disk}}/c_{\text{phot}}$ have been found to lie within the range 1.00 ± 0.01. Thus the two attenuation coefficients are practically equal.

The upward luminances at the surface and the Secchi depth, $L(0)$ and $L(Z_D)$, were found by integrating the spectral upward luminances at the two depths, and then $K_{\text{L, phot}}$ could be determined by using Eq. (9). Because the observed values of Z_D for the black disk were less than for the white disk (Table 3), the spectral luminance $L(Z_D)$ at this smaller depth differed from the former luminance, and accordingly c_{phot} and $K_{\text{L, phot}}$ for the black disk also became slightly different (Table 3). The attenuation coefficients c_{phot} and $K_{\text{L, phot}}$ for the luminances observed through colour filters were calculated in the same way as for the open-eye coefficients.

OSD
10, 1833–1893, 2013

4.2 Values of ρ_{DL}, R_L, $\Re$, $\overline{\rho}_{L,air}$, ln(A_1) and ln(A_2)

It was explained in Sect. 4.1 how the downward illuminance and the reflected luminance from the disk were determined, and how different values of ρ_{DL} obtained by Eq. (6) were found in our laboratory. From the latter recordings ρ_{DL} was estimated equal to 0.30 for the red filter, and by definition equal to 0 for the black disk. The values of ρ_{DL} for the white disk and the blue and green filters were determined by using the spectral recordings of downward illuminance, and the results are 0.29, 0.27 and 0.29, respectively (Table 3).

The mean value of $R_L(0)$, defined as the ratio between upward luminance and downward illuminance just beneath the surface (Eq. 7), has been calculated from 32 stations as 0.56 % for the open eye. This value is valid for both the white and black disks (Table 3). However, the mean value of $R_L(Z_D)$ at the Secchi depth becomes different for the white and black disks, being 0.83 % and 0.61 % respectively, and the reason for this is that Z_D differs for these disks. The estimated values of R_L for the colour filters are shown in Table 3.

It was found by Aas et al. (2009) that an average value for the quantity $\Re$ in the Oslofjord–Skagerrak area was 0.506 ± 0.045 for solar altitudes between 15° and 60°, which is close to similar results found by Morel and Gentili (1996) and Mobley (1999). $\Re$ was assumed to be independent of wavelength, and the found value has been applied for both the white and black disks (Table 3).

The radiance reflected towards the zenith at the surface of the sea is described by the radiance reflectance $\overline{\rho}_{L,air}$. Its value for a clear sky depends on the angular distribution of sky radiance, the solar altitude, the ratio between diffuse sky irradiance and direct solar irradiance, and the statistical distribution of surface slopes. A data set of $\overline{\rho}_{L,air}$ was obtained during a previous work, where the surface reflectance of daylight towards the zenith was estimated (Aas, 2010). The problem was simplified by looking at average values for all possible angles between wind direction and solar azimuth, using the Cox and Munk model with a one-dimensional Gaussian distribution for the surface slopes

OSD
10, 1833–1893, 2013

(Cox and Munk, 1954a, b). The input was spectral sky and solar radiance data from the Oslo region (Høkedal and Aas, 1998; Aas and Høkedal, 1999). However, there is the problem that while the wave height and wave spectrum are functions of wind speed, duration and fetch, only the wind speed appears in the Cox–Munk model. A comparison between wave heights and wind speeds at those of our stations where both quantities were observed, shows that in many cases either the wind duration or the fetch must have had a limiting effect on the wave height. Still the mean values ± the standard errors of wind speed and wave height, $5.5 \pm 0.4\,\mathrm{m\,s^{-1}}$ and $0.7 \pm 0.1\,\mathrm{m}$ respectively, are consistent with the conditions for a fully developed sea shown in the diagram by Gröen and Dorrestein (1976, also shown by WMO, 1998). Accordingly we have tentatively chosen the wind speed $5.5\,\mathrm{m\,s^{-1}}$ to represent the average conditions. The mean values and standard deviations of $\overline{\rho}_{\mathrm{L,\,air}}$ shown in Table 3 are based on 10 different cases of atmospheric radiance distribution. The values of $\overline{\rho}_{\mathrm{L,\,air}}$ for the open eye (the white and black disks) and for the blue, green and red filters were obtained from atmospheric radiance distributions at 550, 470, 540 and 620 nm, respectively (Table 3).

The estimated mean value and standard deviation of $\ln(A_1)$ were obtained by using the value of ρ_{DL} shown in Table 3, and varying values of $R_{\mathrm{L}}(Z_{\mathrm{D}})$ for each station. Similarly the values of $\ln(A_2)$ were found from the values of $\overline{\rho}_{\mathrm{L,\,air}}$ and $\mathfrak{R}$ suggested by Table 3 and varying values of $R_{\mathrm{L}}(0)$. The results for $\ln(A_1)$ and $\ln(A_2)$ are presented in Table 3.

The size distributions of the optical quantities estimated here are often highly asymmetric, implying that the standard deviation does not always provide a satisfactory description of the range of variation, like when the standard deviation is greater than the mean value.

4.3 Value of C_{t} and W

According to Blackwell (1946) the contrast threshold C_{t} depends on the angle α subtended by the observed target, the luminance $L(0)$ of the background, and the probability of detection. C_{t} decreases with increasing α and increasing $L(0)$, and increases

OSD
10, 1833–1893, 2013

with increasing detection probability. In Part I of Blackwell's investigation circular targets, brighter than the background, had an exposure time of six seconds, and the contrast thresholds were those that corresponded to a 50 % detection probability. In Part II the targets were darker than the background, and the conclusion was that in most cases negative stimuli are equivalent to positive stimuli of the same area and contrast. The results in Part III were obtained when an indefinitely long exposure time was used. A comparison between Blackwell's experiments and Secchi disk observations is not straightforward, because Blackwell's target images were constant during the time of exposure, while at sea the image of the Secchi disk is usually varying. We have chosen an indefinitely long exposure time and the highest detection probability, 100 %.

The apparent angle α from the observer's eye across the Secchi disk is a function of the diameter D of the disk, the height H of the observer's eye above the surface of the sea, the Secchi depth Z_D and the refractive index n. Because α is a small angle, $\tan(\alpha/2)$ can be approximated by $\alpha/2$, and $\tan(j)$, where j is the corresponding angle of refraction in water, can be approximated by $\alpha/(2n)$, using Snell's Law. The angle α in radians becomes

$$\alpha = \frac{D}{H + (Z_D/n)} \tag{22}$$

If we use Eq. (22) with $D = 0.3$ m, $H = 3$ m, $n = 1.33$, and if Z_D lies in the interval from 0.5 to 14 m, then the angle α across the Secchi disk will lie between 1.3° and 5.1°. This is within the range in Blackwell's study where the angles of α extended from 0.01° to 6°. Our recordings showed that the background luminances $L(0)$ in the Oslofjord–Skagerrak area were in the range 0.4–1600 cd m^{-2} for the observations with open eye and colour filters. Blackwell's luminances extended from 3×10^{-6} to 3400 cd m^{-2}. Thus our environmental conditions were within the ranges described by Blackwell's experiments. We have selected those of Blackwell's data that are closest to our observed background luminances and angles of subtense, and interpolated these data to fit our

OSD
10, 1833–1893, 2013

ranges. The estimated mean values of C_t and $\ln(C_t)$ for the 30 cm disk, observed with the open eye and through colour filters are presented in Table 3.

Rather than calculating C_t for each single case and then finding the mean value and standard deviation from the resulting data set, we have found it necessary to restrict the calculations of C_t to the mean, maximum and minimum conditions. The mean conditions were assumed to produce the mean value of C_t, and a crude estimate of the standard deviation was obtained by the expression $(C_{t,\max} - C_{t,\min})/4$. For a normal distribution, 95 % of the observations will fall within a range of ±2 standard deviations from the mean value.

In Table 3 the mean value of C_t is 0.56 % for the white disk, and the mean value of $\ln(C_t)$ becomes −5.2. Krümmel (1889) referred to Helmholtz for the threshold contrast $1/133 = 0.75$ % which produces $\ln(C_t) = -4.9$. The relative difference between the last number and our estimate is only 6 %. Tyler (1968) applied $C_t \approx 0.66$ %, leading to $\ln(C_t) = -5.0$, which is even closer to our estimate. Gordon and Wouters (1978) applied C_t values from 0.15 to 0.6 % or $\ln(C_t)$ from −5.1 to −6.5 in their model studies. Højerslev (1986) deduced from his Baltic recordings a threshold contrast slightly greater than our estimate, $C_t = (0.70 \pm 0.03)$ %, resulting in $\ln(C_t) = -(4.96 \pm 0.04)$. Considering that C_t is not supposed to be a constant, these values are surprisingly similar.

It is noteworthy that Blackwell's experiments involved both the colour and night visions of the human eye. It is well known that the night vision requires some time to be activated and adapted, and that a sudden bright glint may temporarily change the vision from night to colour mode. The range where both colour and night visions are active, termed mesopic vision, is 0.001–10 cd m^{-2} according to the CIE. Thus some of our colour filter observations are within this range, but to which extent the varying light conditions have influenced the resulting Secchi depths, we cannot say.

Since our Secchi depths usually are from coastal areas where the surrounding land masses reduce the influence of the wind on the ordinary sea waves, the use of Eq. (14) may perhaps also be overestimating the effect of the wind on the capillary waves. Still we have tentatively estimated W by using the observed wind speeds and Secchi

OSD
10, 1833–1893, 2013

depths. The average values of W and $\ln(W)$, based on the 32 stations constituting the data set where we have complete observations of c, K_L and R_L, are shown in Table 3.

4.4 Value of $\ln(A)$ and comparison to observations of $Z_{D,\,white}(c + K_L)_{phot}$

There are different ways to test Eq. (21) and to estimate a value for $\ln(A)$, and the result will depend on the chosen method. By using the estimated mean values of $\ln(A_1)$, $\ln(A_2)$, $\ln(W)$ and $\ln(C_t)$ from Table 3, $\ln(A)$ in Eq. (21) obtains the value 7.3 for the 30 cm white disk. The left hand side of the equation is the expression $Z_{D,\,white}(c + K_L)_{phot}$, and its mean value found from observations is 7.0 (Table 3), which is 4 % less than the predicted value. Early in the analysis it was discovered that whenever $Z_{D,\,white}$ was in the range 1–2 m, the values of $Z_{D,\,white}(c + K_L)_{phot}$ tended to increase to 10–14, and consequently the few stations where $Z_{D,\,white} < 2$ m have been omitted. The reason for the discrepancy between theory and observations for small Secchi depths may be that one or more of the assumptions on which Eq. (21) is based, becomes invalid. For instance the assumption $L_{*D}(z) \approx L_*(z)$ made for Eq. (4) may be less good when Z_D is small. Figure 2 presents $(c + K_L)_{phot}$ as a function of $Z_{D,\,white}$ at the 32 stations where we have sufficient observations down to the Secchi depth, with the curve

$$(c + K_L)_{phot} = \frac{7.0}{Z_{D,\,white}} \tag{23}$$

added. Another way to test Eq. (21) is to correlate $(c + K_L)_{phot}$ to $1/Z_{D,\,white}$. The best-fit line through the origin obtains the slope 7.5, and if $(c + K_L)_{phot}$ is estimated by $7.5/Z_{D,\,white}$, the rms of the error $[(c + K_L)_{phot} - 7.5/Z_{D,\,white}]$ becomes 0.23 m^{-1}. The mean value of $(c + K_L)_{phot}$ is 1.09 m^{-1} (Table 3), and the rms error relative to this value represents 21 %. It is interesting that if we estimate $(c + K_L)_{phot}$ by using Eq. (23), the rms error only changes to 0.24 m^{-1} or 22 %.

If the observer's eye is below the surface, $\overline{\rho}_{L,\,air} = 0$ and $W = 1$, and the value of $\ln(A)$ in Eq. (21) becomes 8.7. Tyler (1968) estimated the number 8.69 for this case, while

OSD
10, 1833–1893, 2013

Holmes (1970) found for sub-surface observations in turbid coastal waters that the average value of $Z_{D,\,white}(c+K_L)_{phot}$ was 9.4. Højerslev (1977) obtained the same value for the sub-surface case. Thus our theoretical estimate of ln(A) for the sub-surface case agrees with Tyler, but deviates 8 % from the estimates by Holmes and Højerslev. Højerslev (1977) found that for observations above the surface, the product $Z_{D,\,white}(c+K_L)_{phot}$ should be in the range 7.9–9.4. This is 8–29 % above our estimate in Table 3.

4.5 Effect of colour filters and the black disk

When the white Secchi disk is observed through the coloured glass filters, the optical coefficients and ln(A) change values, as shown by Table 3. The table demonstrates that in this case the observed mean values of $Z_D(c+K_L)_{phot}$ are more than 30 % smaller than the estimated mean values of ln(A).

The best-fit correlation lines $y = A + Bx$ and $y = B_0x$ for the observations of $Z_{D,\,blue}$, $Z_{D,\,green}$ and $Z_{D,\,red}$ as functions of $Z_{D,\,white}$ have been determined, and the found constants A, B and B_0 as well as the mean values of the ratios $(y/x) = Z_{D,\,filter}/Z_{D,\,white}$ are presented in Table 4. We see that the colour filters reduce the Secchi depths to 50–70 % of the depths for the open eye. The result that $Z_{D,\,green}$ on an average is reduced to almost 70 % of $Z_{D,\,white}$, although the wavelengths of peak photopic sensitivity for $Z_{D,\,green}$ and $Z_{D,\,white}$ are very close (Table 2), may be due to the half-peak bandwidth of the green filter which is only half of that for the open eye.

Table 4 also shows the correlation lines $y = A + Bx$ with the constant term A. When the values of B_0, B and $(y/x)_{mean}$ are close to each other, it means that the observations lie close to a straight line through the origin.

Mikaelsen and Aas (1990) observed the Secchi depth in the Inner Oslofjord during 1986–87. Based on their data from 11 stations the mean values of the ratio $Z_{D,\,filter}/Z_{D,\,white}$ become 0.61, 0.81 and 0.62 for the blue, green and red filter, respectively, which is 11–15 % greater than our results of 0.53, 0.73 and 0.54 in Table 4. Both the first and the latter set of values resemble Lisitzin's results from the Baltic Sea (1938) when $Z_{D,\,white} < 10$ m. In the clear and blue waters of the Florida Shelf where $Z_{D,\,white}$

OSD
10, 1833–1893, 2013

was 21–26 m, Højerslev's colour filter observations (1985) yielded mean values of the ratios equal to 0.90, 0.91 and 0.29 for the blue, green and red filters. The difference from our results in greenish coastal waters is clearly a result of the difference in water colour.

Table 3 predicts that the average value of $Z_{\mathrm{D,\,black}}(c + K_L)_{\mathrm{phot}}$ should be $\ln(A) = 4.7$ for the 30 cm black disk, but the observed value is less than half of this: 1.9. This could be because an ordinary disk of black plastic was used in these observations, and not the bowl-shaped device. The surface of the plastic disk seemed to be entirely black on deck, but looked dark grey in the sea, and brighter than its background. In 1992 a series of measurements at 19 stations was taken with the black-painted bowl together with the black and white disks. The depth $Z_{\mathrm{B,\,black}}$ of the black bowl was on an average 20–30 % greater than the depth $Z_{\mathrm{D,\,black}}$ of the black disk (Table 4). Thus the bowl produces a smaller reflection and a greater contrast than the disk. Since the estimated attenuation $(c + K_L)_{\mathrm{phot}}$ is approximately the same for the black and white disks as shown by Table 3 (the minor difference being due to $Z_{\mathrm{D,\,black}}$ being smaller than $Z_{\mathrm{D,\,white}}$), the values of $\ln(A)$ in Table 3 imply that the ratio $Z_{\mathrm{B,\,black}}/Z_{\mathrm{D,\,white}}$ should be approximately $4.7/7.3 = 0.64$. However, the observed ratio in Table 4 is only 0.23–0.26. This could mean that our black bowl is not perfectly black, but it could also be that the use of colour filters and the black disk or bowl introduces effects that is not included in Eq. (21).

4.6 Effect of size

The observations with the 10 cm disks were made in 1992, when instruments for spectral recordings of c and K_L were not available. Consequently the two sides of Eq. (21) cannot be tested directly for the 10 cm disk, but other experiments have been made. The angle α of the total field of view across the 10 cm Secchi disk can be calculated from Eq. (22) with $D = 0.1$ m, $H = 3$ m and $n = 1.33$. Because the observed values of Z_{D} for this smaller disk lie in the interval from 0.5 to 12 m, the angle α across the Secchi disk becomes 0.5–1.7°. The threshold contrast for the smaller disk becomes greater

OSD
10, 1833–1893, 2013

than for the 30 cm disk, while the value of W will be reduced according to Eq. (14), because D^2 is reduced more than Z_D^2. The combined effect is that the values of ln(A) in Table 3 for the 30 cm white and black disks will be reduced by 22 and 13 %, respectively. For the blue, green and red colour filters the decreased size produces similar reductions of 18, 21, and 17 %. This can be tested directly by comparing the values of Z_D for disk diameters of 10 and 30 cm. The results in Table 4 show that the relative influence of size is greater for the open eye than for the colour filters, and that the decrease of diameter from 30 to 10 cm reduces the Secchi depth on an average by 10–20 %, in agreement with our estimates. Figure 3 presents all open eye and colour filter observations for 10 and 30 cm disks put together, and the best fit line through the origin obtains a slope of 0.83, indicating an average Secchi depth reduction of 17 %.

4.7 Effects of sun glitter, water telescope and ship shadow

The effect of a water telescope is to eliminate sun glitter and skylight reflection at the surface, and to reduce the blurring effect of capillary waves. If we insert a surface reflectance $\overline{\rho}_{L,\,air} = 0$ and a wave factor $W = 1$ in Eq. (21), we find that ln(A) should increase by 12 % for the 30 cm white disk, based on the estimated quantities in Table 3. For the colour filters and black disk the effect is in the range ±6 %. Mikaelsen and Aas (1990) tested the effect at four stations in 1987 with a 30 cm disk. According to their observations $Z_{D,\,white}$ increased by 11 % on an average by using the water telescope, and by including the observations with the colour filters the increase became 15 %. New experiments were made in 1992, and a 10 cm disk was used in order to see it properly within the field of view of the telescope. The results, listed in the last five rows of Table 4, show that the telescope increased $Z_{D,\,white,\,10}$ on an average by 14 %, and the effect on $Z_{D,\,filter,\,10}$ was of the same magnitude. If all open-eye and filter observations are put together (Table 4), we see that the average increase of the Secchi depth by using the telescope is the same, 14 %. The best-fit line through the origin obtains the slope 1.19 (Fig. 4), indicating an average increase of 19 %.

OSD
10, 1833–1893, 2013

Holmes' use of a water telescope (1970) only increased the observed depth by 2–4 %, which is significantly less than our result. Højerslev (1986) found for Baltic waters that the ratio between the depth $Z_{D,\,tel}$ observed with a water telescope and the ordinary Z_D could be approximated by a function of the wave height H in units of meters: $Z_{D,\,tel}/Z_D = 1 + 0.4H$. This expression underestimates the effect at our 11 water telescope stations where H was < 0.1 m, but we have not tested it in more rough sea. Sandén and Håkansson (1996) investigated the effect of wind on Z_D, and it seems like the presence of wind tended to reduce the depth by ~ 10 %.

If we are observing the Secchi disk on the sunlit side of the ship, sun glitter from the sea will reduce its threshold depth. On the shadow side there may be less glitter, but the ship shadow will also reduce the luminances from both the background and the disk, and this may require a greater contrast, and thus lead to a smaller depth. The balance between gains and losses related to the absence or presence of direct sunlight is demonstrated by Fig. 5 which presents the Secchi depths observed on both sides of the ship. The best-fit line through the origin obtains the slope 0.97, which is close to 1. If we make the same experiment for the depths observed with colour filters (Table 4), we see that $Z_{D,\,filter}$ is slightly more reduced on the shadow side than $Z_{D,\,white}$.

5 The monochromatic assumption

In Sect. 2 it was assumed as a first approximation that the beam attenuations of the upward luminances resembled the attenuations of the radiances at the wavelength of maximum spectral transmittance, and Sect. 4.1 described how the efficient attenuation coefficients $c_{phot,\,disk}$ and c_{phot} of upward luminance from the disk and background could be estimated. In this section we will investigate the relationships between the photopic and monochromatic coefficients as well as the errors introduced by the monochromatic assumption.

The coefficients $c_{phot,\,disk}$ and c_{phot} have been correlated to the monochromatic beam attenuation coefficient c_{555} at 555 nm, and the results are presented in Table 5. Simi-

OSD
10, 1833–1893, 2013

larly the vertical attenuation coefficient $K_{L,\,phot}$ has been correlated to $K_{L,\,555}$. The correlations are described by best-fit lines on the forms $y = A + Bx$ and $y = B_0 x$. Table 5 also displays values of $(y/x)_{mean}$ and y_{mean}. We see that the values of B, B_0 and $(y/x)_{mean}$ are close to each other, indicating that the points (y, x) lie close to the lines. This is confirmed by the very small errors ε and ε_0 introduced by using the correlation lines ($\approx 0.01\,m^{-1}$). ε and ε_0 are defined as the root-mean-squares of the deviations $(y - A - Bx)$ and $(y - B_0 x)$, respectively. The coefficients c_{phot}, for instance, is almost identical to c_{555}, with an average ratio of 1.02. However, Table 5 also demonstrates that the deviations between the photic and monochromatic coefficients are greatest for $K_{L,\,phot}$ vs. $K_{L,\,555}$ which displays a slope of 1.12. The sum $(c + K_L)_{phot}$ vs. $(c + K_L)_{555}$ obtains the slope 1.03.

It follows from the descriptions of c_{phot} and $K_{L,\,phot}$ that these coefficients are apparent optical properties, depending on the ambient light field. It could not be stated a priori that they would be so strongly correlated to the monochromatic coefficients at 555 nm, with a coefficient of correlation equal to 1.00. We have not investigated how the found relationships will work in more clear and bluish sea waters, but we assume that the correlations may be weaker there. Holmes (1970) equipped his irradiance and beam attenuation meters with filters where the spectral shape of the transmittance resembled the spectral sensitivity of the eye, but the attenuation meter then recorded a lamp spectrum that probably was different from the natural spectrum within the sea.

The correlation results for attenuation coefficients derived from luminances observed through the colour filters (Table 5) vs. monochromatic coefficients show that the correlation coefficients are all very close to 1.0. The slope B_0 for the blue and green filters obtains values between 0.95 and 1.01, while the red filter deviates more from 1.0 with the slopes 1.06 and 1.21. The slopes B_0 for the sum $(c + K_L)$ are in the range 0.97–1.10. None of these deviations from the slope 1.0 explain the discrepancies between theory and observations displayed by Table 3 for the colour filters. Our overall conclusion becomes that the monochromatic assumption works satisfactorily, and that the mentioned discrepancies must have other causes. In Blackwell's experiments (1946) the targets

OSD
10, 1833–1893, 2013

were projections of "white" light from electrical lamps onto a white screen. The different parts of the visible spectrum were not investigated separately, and it could perhaps be that C_t also has a spectral dependence.

It remains to test the ability of Eq. (21) to describe the relationships between Z_D and monochromatic values of c, K_L and $(c + K_L)$. This will be done in the next section.

6 Further analyses of the Secchi depths

6.1 Estimates of monochromatic coefficients

In Sect. 2 we assumed that the Secchi depth observed with the open eye might be determined by the attenuation coefficients at the wavelength of maximum water transmittance, that is around 555 nm (Table 1a, b). Section 4.4 demonstrated that the numerical values of the constants in the relationships between Z_D and $(c + K_L)$ would depend on the chosen method. If our intention is to estimate $(c + K_L)_{555}$ from observed $Z_{D,\,white}$, the obvious choice, based on the form of Eq. (21), is to perform a linear correlation analysis between $(c + K_L)_{555}$ and $1/Z_{D,\,white}$. The slope of the line through the origin obtains the value 7.4, which is practically the same as the slope 7.5 found in Sect. 4.4 for $(c + K_L)_{phot}$. However, usually in marine-optical research the singular values of c and K_L are more interesting than their sum $(c + K_L)$, and therefore c_{555} and $K_{L,\,555}$ have been separately correlated to $1/Z_{D,\,white}$, as shown by Table 6. While the correlation coefficient is 0.95 for c_{555}, which is almost as perfect as it can be expected to be, it is reduced to 0.72 for $K_{L,\,555}$. Similar results have been obtained for the channels at 412, 443, 490, 510, 620 and 665 nm (Table 6). The root-mean-square errors of K_L and c, estimated from the correlation lines, are in the range 0.1–0.6 m^{-1}, but because K_L is smaller than c the relative errors become greater for K_L than for c. The result that the correlation coefficients are greater for c than for K_L is as expected since c contributes more than K_L to the sum $(c + K_L)$ which determines $Z_{D,\,white}$.

OSD
10, 1833–1893, 2013

Often the vertical attenuation coefficient of downward irradiance, K_d, will be a more useful quantity than K_L. The correlation results for K_d at the MERIS channels as a function of $1/Z_{D,\,white}$ are presented in Table 6. Some of the values are remarkably similar to those obtained for K_L, and the reason for this is that the mean value of the ratio K_d/K_L usually is close to 1. In order to complete the investigation, the coefficient K_u of upward irradiance has been included in Table 6. The results indicate that the errors of the estimated vertical coefficients are greatest for K_u and smallest for K_L, and less in the green and red part of the spectrum than in the blue part. We suspect that the rms errors at 412 and 443 nm of 90–100 % are due to varying amounts of yellow substance which will influence the coefficients more than the Secchi depth. In addition weak signals compared to noise and detection level at these wavelengths create errors.

Gordon and Wouters (1978) found in their model study that in relatively turbid water, defined by the authors as water where the backscattering probability is constant, the product $cZ_{D,\,white}$ would be approximately constant, while $(c + K_d)Z_{D,\,white}$ would vary more. This result is in agreement with the results in Table 6.

In Table 6 the errors of the estimates produced by the best-fit lines $y = A + Bx$ and $y = B_0x$, where y is an attenuation coefficient and $x = 1/Z_{D,\,white}$, are shown. Usually the line $y = B_0x$ through the origin works satisfactorily, but at some wavelengths the addition of a constant term A reduces the error of the estimates significantly. Figure 6 shows observations of K_d at 555 and 665 nm vs. $x = 1/Z_{D,\,white}$, together with the best-fit lines $y = A + Bx$. The value of A is 0.02 m^{-1} at 555 nm, and 0.41 m^{-1} at 665 nm (Table 6). It is interesting that Jerlov's K_d values for the clearest ocean water type I are of the same order of magnitude: 0.07 m^{-1} at 555 nm and 0.40 m^{-1} at 665 nm (e.g. Jerlov, 1976). Figure 6 indicates that in the green part of the spectrum the constant term can be omitted without any practical consequences, while in the red part a better fit is obtained if A is included. The inclusion of the constant term A reduces the error at 665 nm from 0.21 m^{-1} to 0.07 m^{-1} according to Table 6. For the vertical attenuation coefficients K_L and K_u of upward directed light the improvements by adding a constant term A to the correlation lines are less.

OSD
10, 1833–1893, 2013

Mikaelsen and Aas (1990) analysed 5 stations in the Oslofjord with recordings of c, and 11 stations with K_d. Z_D was observed by the naked eye and with colour filters. Most of their results overlap with the present findings. Sørensen et al. (1993) obtained from 189 stations in the Oslofjord–Skagerrak area the mean value and standard deviation $c_{green} Z_{D,\,white} = 6.2 \pm 1.3$, which falls within the corresponding range of Table 6.

The relationships between the Secchi depths observed through the glass filters and the coefficients c, K_L, K_d and K_u at 470, 540 and 620 nm are presented in Table 7. The results, based on 25 stations, show that the errors of the estimated coefficients are in the range 0.07–0.47 m^{-1}, or 10–80 % of the corresponding mean values. It is noteworthy that compared to the observations with the open eye, the colour filter observations represent no improvement of the accuracy of the estimated vertical attenuation coefficients. Especially for the coefficients of beam attenuation it is clear that $Z_{D,\,white}$ produces better estimates than $Z_{D,\,filter}$. We think this result is valid within our area of investigation, but not necessarily in other sea regions.

It may be noted that Table 7 contains analyses of attenuation coefficients at 620 nm that are parallel to those in Table 6, and that the results are different. The reason for this may be that Table 7 is based on stations with colour filter observations, and accordingly the number of applicable stations will be reduced to less than half of those in Table 6. Evidently the number of stations influences the statistical results.

Højerslev (1977) suggested the approximate mean values 3, 6 and 9 for the products $K_d Z_D$, $c Z_D$ and $(c+K_d) Z_D$, respectively, where K_d, c and Z_D are observed through colour filters, but these findings are not confirmed by Table 7.

Because remote sensing of ocean colour is used to estimate coefficients like K_d, the technique can also be used to estimate the Secchi depth. Within our area of investigation the relationship between $1/Z_{D,\,white}$ and the water-leaving radiance L_w recorded in the red part of the spectrum (630–690 nm) by the TM3 sensor at the Landsat satellite was found to be $1/Z_{D,\,white} = [0.203\,m^{-1}] + [0.072\,W^{-1}\,m\,sr\,\mu m] L_w$, while the coefficient of correlation was 0.92 (Sørensen and Aas, 1994). For the TM1, TM2 and TM4 sensors in the blue-green (450–520 nm), green (520–600 nm) and near-infrared (760–900 nm)

OSD
10, 1833–1893, 2013

parts of the spectrum the coefficients of correlation became 0.69, 0.87 and 0.65, respectively. Kratzer et al. (2003) and Zhang et al. (2003) have discussed estimates of $1/Z_{D,\,white}$ based on satellite observation of the Baltic Sea, and Morel et al. (2007) have examined the Secchi depth estimates from various ocean colour sensors for the open ocean case. References to numerous investigations in lake waters can be found on the internet.

6.2 Quanta irradiance – PAR

The spectrally integrated quanta irradiance (400–750 nm), also termed PAR (Photosynthetically Available Radiation), is one of several factors determining the primary production in the sea. If the transmittance of this irradiance between the surface and the Secchi depth is denoted T_D, then the average vertical attenuation coefficient K_q of the irradiance over the depth range $0 - Z_{D,\,white}$ is related to $Z_{D,\,white}$ by

$$T_D = e^{-K_q Z_{D,\,white}} \tag{24}$$

The observed mean value ± the standard deviation of T_D, obtained from our third data set of 143 stations from the Oslofjord inside the Færder Light House at the Skagerrak border, is (9 ± 4) %. Based on the total data set of 205 stations, including stations from the nearby Skagerrak and Kattegat, the range becomes slightly greater: (9 ± 6) %.

Equation (24) can also be written

$$K_q Z_{D,\,white} = -\ln(T_D) \tag{25}$$

and by using $T_D \approx 0.09 \pm 0.06$, the range of the product $K_q Z_{D,\,white}$ becomes 1.9–3.5. This is consistent with the mean value and standard deviation of the product obtained from observed pairs of K_q and $Z_{D,\,white}$: 2.5 ± 0.5 (Table 8). By linear correlation K_q may be estimated from $1/Z_{D,\,white}$ with an rms error that is less than 20 % of the mean value of K_q.

OSD
10, 1833–1893, 2013

The depth of the euphotic zone, defined as the surface layer where there is a net positive production from photosynthesis, is often estimated as the depth $Z_q(1\,\%)$ where the quanta irradiance is reduced to 1 % of its surface value. If K_q is approximately constant with depth, $Z_q(1\,\%)$ can be determined from the equation

$$0.01 = e^{-K_q Z_q(1\,\%)} \tag{26}$$

which can be transformed to

$$Z_q(1\,\%) = \frac{4.61}{K_q} \tag{27}$$

By inserting for K_q from Eq. (25), this expression becomes

$$Z_q(1\,\%) = \frac{4.61}{-\ln(T_D)} Z_{D,\,white} \tag{28}$$

indicating a linear proportionality between $Z_q(1\,\%)$ and $Z_{D,\,white}$, provided $\ln(T_D)$ is approximately constant. Similar expressions can be deduced for $Z_q(3\,\%)$, $Z_q(10\,\%)$ and$Z_q(30\,\%)$.The correlation results for $Z_q(p\%)$ as a function of $Z_{D,\,white}$ are presented in Table 8, together with other related statistics.

An old rule of thumb for the Oslofjord says that $Z_q(10\,\%)$ corresponds roughly to $Z_{D,\,white}$ (also suggested by Paulson and Simpson, 1977), and $Z_q(1\,\%)$ to twice this depth. We have already found that the average percentage of the quanta irradiance at $Z_{D,\,white}$ was 9 %, and when we calculate the average ratios $Z_q(10\,\%)/Z_{D,\,white}$ and $Z_q(1\,\%)/Z_{D,\,white}$, they become 0.9 and 2.2, respectively (Table 8). Figure 7 illustrates the significant scattering of points around the correlation line through the origin for $Z_q(1\,\%)$ as a function of $Z_{D,\,white}$. If we apply the relationship $y = A + Bx$ instead of the line through the origin, a slightly better fit is obtained, and the rms error for the esimates of $Z_q(1\,\%)$ as a function of $Z_{D,\,white}$ is reduced from 3.1 to 2.7 m (Table 8). Compared to the mean value 11.5 m of $Z_q(1\,\%)$, these numbers represent relative errors of 27 and 23 %, respectively.

OSD
10, 1833–1893, 2013

Table 8 shows that estimates of Z_q from observed $Z_{D,\,white}$ are likely to have relative mean errors in the range 20–30 %. This is because $Z_{D,\,white}$ is primarily a function of $c + K_L$ (Eq. 20), while Z_q is a function of K_q only (Eq. 27). The vertical attenuation coefficients K_L and K_q are mainly functions of the absorption coefficient a, while the beam attenuation coefficient c consists of $a + b$, where b is the scattering coefficient. Thus Z_q is less influenced by particle scattering than Z_D, a property which reduces the correlation between the two quantities. It is our experience that an increased particle content in the sea may have a strong reducing effect on Z_D, while the influence on Z_q is much smaller. Still the relationships in Table 8 will provide very useful checks of our irradiance measurements.

Not surprisingly the inter-correlations between $Z_q(1\,\%)$, $Z_q(3\,\%)$, $Z_q(10\,\%)$ and $Z_q(30\,\%)$ are stronger than between Z_q and $Z_{D,\,white}$ (Fig. 8). The statistical relationships are shown in Table 8.

Mikaelsen and Aas (1990) found $K_q Z_{D,\,white} = 2.7 \pm 0.6$, $Z_q(10\,\%) = 0.66 Z_{D,\,white}$ and $Z_q(1\,\%) = 1.7 Z_{D,\,white}$, while Sørensen et al. (1993) obtained $K_q Z_{D,\,white} = 2.3 \pm 0.4$. All of these results are close to the values in Table 8. Kratzer et al. (2003) found for Baltic waters that $K_q \approx 1.7/Z_{D,\,white}$, implying that for the same K_q the Secchi depth $Z_{D,\,white}$ tends to be greater in the Oslofjord than in the Baltic.

6.3 Chlorophyll *a* and total suspended material

The chlorophyll content is perhaps the most used concept when the amount of algae in the sea shall be described. Unfortunately the concentration of chlorophyll *a* (Chl) is not an optical property, although it influences the absorption and scattering coefficients of sea water. As a result our estimates obtained by correlation analysis of Chl as a function of $1/Z_D$, based on 19 stations, have average errors of 30–40 % (Table 9).

Even less accurate are the estimates of total suspended material (TSM), with average errors of approximately 50 % (Table 9). Still such relationships provide useful checks because they quantify the order of magnitude of the concentrations.

OSD
10, 1833–1893, 2013

In the earlier investigation by Sørensen et al. (1993) the products $Z_{D,\,white}$Chl (249 stations) and $Z_{D,\,white}$TSM (275 stations) obtained the mean values and standard deviations $(19 \pm 16)\,mg\,m^{-2}$ and $(7.8 \pm 3.8)\,g\,m^{-2}$, respectively, in agreement with the corresponding ranges of Table 9. An estimate of the product $Z_{D,\,white}$Chl in the Baltic Sea, based on observations by Fleming-Lehtinen and Laamanen (2012), is $\sim 25\,mg\,m^{-2}$.

The turbidity Turb, expressed in nephelometric formazine units (NFU), has not been included in the present study, because the accuracy of the corresponding turbidity data was not satisfactory. However, in the mentioned investigation by Sørensen et al. (1993) the product $Z_{D,\,white}$Turb (308 stations) was (3.5 ± 1.4) m NFU.

7 Summary and conclusions

We have analyzed the Secchi depth Z_D and its relationship to other properties of the sea water in the Oslofjord–Skagerrak area. White and black disks of different sizes have been applied, and the Secchi depth has been observed with the naked eye, through colour filters and with a water telescope. A few stations where $Z_{D,\,white}$ was less than 2 m or the Q factor was outside the range π–2π, have been omitted. The upward luminance will typically have its spectral maximum in the green part of the spectrum, close to 555 nm (Table 1b).

An extended version of Tyler's equation for Z_D, as expressed by Eq. (21), has been tested. The right hand side of the equation, $\ln(A)$, is a function of the reflectance $\overline{\rho}_{L,\,air}$ at the air–sea interface, the reflectances $R_L(0)$ and $R_L(Z_D)$ of the sea water just below the surface and at the Secchi depth, the reflectance ρ_{DL} of the disk, the contrast threshold C_t of the human eye, the contrast transmittance W through the surface and the factor $\Re$. With the estimated mean values for these quantities (Table 3), $\ln(A)$ obtains the mean value ± the standard deviation 7.3 ± 0.9 for the 30 cm white disk observed with the naked eye. The left hand side of the equation is the product of the observed Secchi depth $Z_{D,\,white}$ and the attenuation coefficients $(c + K_L)_{phot}$, and its mean value becomes 7.0 ± 1.3 (Table 3, Fig. 2). Thus on an average the observed value is only 4 % less

OSD
10, 1833–1893, 2013

than the predicted one for the white disk. The slope of the best-fit line through the origin for $(c + K_L)_{\text{phot}}$ as a function of $1/Z_{\text{D, white}}$ becomes 7.5. The deviation between the observed $(c+K_L)_{\text{phot}}$ and its estimate $7.5/Z_{\text{D, white}}$ obtains an rms value of 0.23 m^{-1}, which represents 21 % of the mean value of $(c + K_L)_{\text{phot}}$ (Table 3).

The agreement between ln(A) of Eq. (21) and the observed $Z_{\text{D}}(c + K_L)_{\text{phot}}$ that we find for the white disk, is reduced when the Secchi disk is observed through coloured glass filters. In this case the observed mean values of $Z_{\text{D}}(c + K_L)_{\text{phot}}$ are more than 30 % smaller than the estimated mean values of ln(A) (Table 3). We speculate if there may be a spectral dependence of C_{t}.

Also the observed depths $Z_{\text{D, black}}$ of the black disk and the related products $Z_{\text{D, black}}(c + K_L)_{\text{phot}}$ were smaller than predicted. According to Table 3 the average value of $Z_{\text{D, black}}(c + K_L)_{\text{phot}}$ should be equal to ln(A) = 4.7 for the 30 cm black disk, but the observed mean value is only 40 % of this. Observations with a black bowl, $Z_{\text{B, black}}$, resulted in 20–30 % greater depths than with the black disk, but the product $Z_{\text{B, black}}(c + K_L)_{\text{phot}}$ is still less than half of the predicted value. One explanation for the deviation could be that the black bowl is not perfectly black. It could also be that the use of colour filters and a black disk or bowl introduces effects that we have not included in ln(A).

If the diameters of the white and black disks are reduced from 30 to 10 cm, the values of C_{t} and W will change, and the corresponding Secchi depths including colour filter observations are predicted by the right hand side of Eq. (21) to be reduced within the range 13–22 %. The observations show that the decrease in size reduces the Secchi depth on an average by 10–20 %, in agreement with this theoretical estimate (Table 4). The best-fit line through the origin for all depths of the 10 cm disk as a function of the depths of the 30 cm disk obtains a slope of 0.83 (Fig. 3), indicating an average Secchi depth reduction of 17 % for the 10 cm disk.

The use of a telescope changes $\overline{\rho}_{\text{L, air}}$ to 0 and W to 1, and according to Eq. (21) the depth of the 30 cm white disk should then increase by 12 %. A few earlier observations confirm this estimate. Experiments made with a 10 cm disk (Table 4) show that the tele-

OSD
10, 1833–1893, 2013

scope increases $Z_{D,\,white,\,10}$ on an average by 14 %, and that the effect on $Z_{D,\,filter,\,10}$ is of the same order of magnitude. If all open-eye and filter observations are put together (Fig. 4), the best-fit line through the origin obtains the slope 1.19. Thus we may state, based on Table 4, that the use of a telescope increases Z_D within the range 10–20 %.

There is practically no difference between observations of the white Secchi disk on the sunlit and shadow sides of the ship (Fig. 5), while the depths observed with colour filters may be reduced by up to 17 % on the shadow side (Table 4).

The mean value ± the standard deviation of the ratio $(c+K_L)_{phot}/(c+K_L)_{555}$ becomes 1.03 ± 0.01, supporting our assumption in Sect. 2 about the monochromatic character of the photopic coefficients. Similarly the ratios c_{phot}/c_{555} and $c_{phot,\,disk}/c_{555}$ are both 1.02 ± 0.01, while the mean value and standard deviation of $K_{L,\,phot}/K_{L,\,555}$ are greater, 1.11 ± 0.05 (Table 5). The attenuation coefficients $c_{phot,\,filter}$ and $K_{L,\,filter}$ derived from luminances observed through colour filters are strongly correlated to the corresponding monochromatic coefficients with correlation coefficients very close to 1.0 (Table 5). The slope of the best-fit line through the origin for the blue and green filters obtains values between 0.95 and 1.01, while the red filter deviates more from 1.0 with the slopes 1.06 and 1.21. Thus our conclusion is that the monochromatic assumption works satisfactorily.

The correlation coefficient r is 0.95 for the linear relationship between c_{555} and $1/Z_{D,\,white}$, while r is reduced to 0.72 for $K_{L,\,555}$ as a function of $1/Z_{D,\,white}$ (Table 6). Similar results are found for the other MERIS channels at 412, 443, 490, 510, 620 and 665 nm. While r is in the range 0.86–0.95 for c, it is reduced to the range 0.66–0.78 for K_L. This result is reasonable since c contributes more than K_L to the sum $(c + K_L)$ which determines $Z_{D,\,white}$. The correlation coefficients for K_d as a function of $1/Z_{D,\,white}$ at the MERIS channels are in the range 0.59–0.86, and for K_u in the range 0.43–0.72 (Table 6). The errors of the estimated vertical coefficients are greatest for K_u and smallest for K_L. In the blue and green parts of the spectrum there are no significant differences between the best-fit line through the origin and the line with a constant

OSD
10, 1833–1893, 2013

term. At 665 nm, however, the introduction of a constant term reduces the rms error from 0.21 m^{-1} to 0.07 m^{-1} (Fig. 6).

Linear relationships between the Secchi depths observed through glass filters and the coefficients c, K_L, K_d and K_u at the wavelengths of peak visual sensitivity at 470, 540 and 620 nm (Table 2) have also been calculated (Table 7). The rms errors of the estimated coefficients are in the range 0.07–0.47 m^{-1}, or 10–80 % of the corresponding mean values. The accuracy of the estimates based on the white disk and naked eye is equal to or better than the estimates from colour filter observations.

The mean vertical attenuation coefficient of quanta irradiance or PAR between the surface and the Secchi depth, K_q, may be estimated from $1/Z_{D,\,white}$ with an rms error less than 20 % of the mean value of K_q (Table 8). The mean values of the ratios $Z_q(10\,\%)/Z_{D,\,white}$ and $Z_q(1\,\%)/Z_{D,\,white}$ are 0.9 and 2.2, respectively, or very close to 1 and 2. Table 8 shows that estimates of Z_q from observed $Z_{D,\,white}$ will have relative errors in the range 20–30 %. The depth of the euphotic zone may be defined as $Z_q(1\,\%)$ (Fig. 7), and according to Table 8 this depth can be estimated by an rms error of 23 %. Consequently these relationships will provide very useful checks of our irradiance measurements. Relationships for $Z_q(3\,\%)$, $Z_q(10\,\%)$ and $Z_q(30\,\%)$ as functions of $Z_q(1\,\%)$, are presented in Fig. 8 and Table 8.

The Secchi depth may also be used to estimate the concentrations of chlorophyll *a* (Chl) and total suspended material (TSM). The estimates of Chl and TSM as functions of $1/Z_D$ have average errors of 30–40 % and 50 %, respectively (Table 9). Still these estimates will provide the order of magnitude of the concentrations.

Our overall conclusion becomes that Eq. (21) quantifies well the relationships between the white disk and the optical attenuation coefficients, but less so for the colour filters and the black disk. The Secchi depths provide very useful checks of the monochromatic attenuation coefficients and of chlorophyll *a* and total suspended material. We assume that there may be regional differences for the found relationships.

Acknowledgement. The in-water spectral irradiance and radiance data from the Oslofjord–Skagerrak area were collected in 2002–2003, as parts of two validation projects: “Validation of

OSD
10, 1833–1893, 2013

MERIS Data Products" (VAMP) funded by ESA, the Norwegian Space Centre and the Norwegian Institute for Water Research (PRODEX contract no. 14849/00/NL/Sfe(IC)), and the "Regional Validation of MERIS Chlorophyll Products in North Sea Coastal Waters" (REVAMP), funded by an FP5 research contract from the European Commission (Contract No. EVG1-CT-2001-00049).

References

Aarup, T.: Transparency of the North Sea and Baltic Sea – a Secchi depth data mining study, Oceanologia, 44, 323–337, 2002.

Aarup, T., Holt, N., and Højerslev, N. K.: Optical measurements in the North Sea–Baltic Sea transition zone, II: Water mass classification along the Jutland west coast from salinity and spectral irradiance measurements, Cont. Shelf Res., 16, 1343–1353, 1996a.

Aarup, T., Holt, N., and Højerslev, N. K.: Optical measurements in the North Sea–Baltic Sea transition zone. II I. Statistical analysis of bio-optical data from the Eastern North Sea, the Skagerrak and the Kattegat, Cont. Shelf Res., 16, 1355–1377, 1996b.

Aas, E.: Estimates of radiance reflected towards the zenith at the surface of the sea, Ocean Sci., 6, 861–876, doi:10.5194/os-6-861-2010, 2010.

Aas, E. and Højerslev, N. K.: Analysis of underwater radiance observations: apparent optical properties and analytic functions describing the angular radiance distribution, J. Geophys. Res., 104, 8015–8024, 1999.

Aas, E. and Høkedal, J.: Reflection of spectral sky irradiance on the surface of the sea and related properties, Remote Sens. Environ., 70, 181–190, 1999.

Aas, E. and Korsbø, B.: Self-shading effect by radiance meters on upward radiance observed in coastal waters, Limnol. Oceanogr., 42, 968–974, 1997.

Aas, E., Andresen, T., Løyning, T., and Sørgård, E.: The eutrophy situation of the Outer Oslofjord, Project 3.7: Optical observations, SFT (Norw. Environ. Agency) Report 388/90, 50 pp., 1989 (in Norwegian).

Aas, E., Højerslev, N. K., and Høkedal, J.: Conversion of sub-surface reflectances to above-surface MERIS reflectance, Int. J. Remote Sens., 30, 5767–5791, 2009.

Blackwell, H. R.: Contrast thresholds of the human eye, J. Opt. Soc. Am., 36, 624–632, 1946.

OSD
10, 1833–1893, 2013

Boguslawski, G. v.: Handbuch der Ozeanographie, Band I: Räumliche, physikalische und chemische Beschaffenheit der Ozeane, Verlag von J. Engelhorn, Stuttgart, 400 pp., 1884.
Cox, C. and Munk, W.: Statistics of the sea surface derived from sun glitter, J. Mar. Res., 13, 198–227, 1954a.
Cox, C. and Munk, W.: The measurements of the roughness of the sea surface from photographs of the sun's glitter, J. Opt. Soc. Am., 44, 838–850, 1954b.
Davies-Colley, R. J.: Measuring water clarity with a black disc, Limnol. Oceanogr., 33, 616–623, 1988.
Duntley, S. Q.: The visibility of submerged objects, Final Rep., Visibility Lab., Mass. Inst. Tech., 74 pp.1952.
Fleming-Lehtinen, V. and Laamanen, M.: Long-term changes in Secchi depth and the role of phytoplankton in explaining light attenuation in the Baltic Sea, Estuar. Coast. Shelf Sci., 102–103, 1–10, 2012.
Gordon, H. R. and Ding, K.: Self-shading of in-water optical instruments, Limnol. Oceanogr., 37, 491–500, 1992,
Gordon, H. R. and Wouters, A. W., Some relationships between Secchi depth and inherent optical properties of natural waters, Appl. Optics, 17, 3341–3343, 1978.
Gröen P. and Dorrestein, R.: Zeegolven, KNMI Opstellen op Oceanografisch en Maritiem Meteorologisch Gebied, 11, 124 pp., 1976 (in Dutch).
Haltrin, V. I.: Spectral relative clarity of Black and Aegan Seas. Geoscience and Remote Sens. Symp. Proc., IGARSS '98, 1998 IEEE International, 2, 913–915, 1998.
Holmes, R. W.: The Secchi disk in turbid coastal waters, Limnol. Oceanogr., 15, 688–694, 1970.
Hou, W., Lee, Z., and Weidemann, A. D.: Why does the Secchi disk disappear? an imaging perspective, Optics Expr., 15, 2791–2802, 2007.
Højerslev, N. K.: Spectral daylight irradiance and light transmittance in natural waters measured by means of a Secchi Disc only, Int. Council Explor. Sea, C. M. 42, 19 pp., 1977.
Højerslev, N. K.: Daylight measurements appropriate for photosynthetic studies in natural sea waters, J. Cons. int, Explor. Mer., 38, 131–146, 1978.
Højerslev, N. K.: Bio-optical measurements in the Southwest Florida Shelf ecosystem. J. Cons. int. Explor. Mer, 42, 65–82, 1985.
Højerslev, N. K.: Visibility of the sea with special reference to the Secchi disc, Ocean Opt., 637, 294–305, 1986.

OSD
10, 1833–1893, 2013

Højerslev, N. K., Holt, N., and Aarup, T.: Optical measurements in the North Sea–Baltic Sea transition zone. I. On the origin of the deep water in the Kattegat, Cont. Shelf Res., 16, 1329–1342, 1996.
Høkedal, J. and Aas, E.: Observations of spectral sky radiance and solar irradiance, Rep. 103, Dept. Geophys., Univ. Oslo, Oslo, 73 pp., 1998.
Jerlov, N. G.: Marine Optics, Elsevier, Amsterdam, 231 pp., 1976.
Kratzer, S., Håkansson, B., and Sahlin, C.: Assessing Secchi and photic zone depth in the Baltic Sea from satellite data, Ambio, 32, 577–585, 2003.
Krümmel, O.: Der Ozean. Eine Einführung in die allgemeine Meereskunde, edited by: Freytag, G. and Leipzig, F. Tempsky, Prag, 242 pp., 1886.
Krümmel, O.: Bemerkungen über die Durchsichtigkeit des Meerwassers, Ann. d. Hydr. mar. Met., 2, 62–78, 1889.
Krümmel, O.: Handbuch der Ozeanographie. Band I. Die räumlichen, chemischen und physikalischen Verhältnisse des Meeres, Verlag von J. Engelhorn, Stuttgart, 526 pp., 1907.
Levin, I. M.: Theory of the white disk, Izvest. Atmos. Ocean. Phys., 16, 678–683, 1980.
Lisitzin, E.: Über die Durchsichtigkeit des Wassers im nördlichen Teil des Baltischen Meeres, Fennia, 65, 1–22, 1938.
Mikaelsen, B. and Aas, E.: Secchi disk depths and related quantities in the Oslofjord 1986–87, Rep. 77, Dept. Geophys., Univ. Oslo, Oslo, 55 pp., 1990.
Mobley, C. D.: Estimation of the remote-sensing reflectance from above-surface measurements, Appl. Optics, 38, 7442–7455, 1999.
Morel, A. and Gentili, B.: Diffuse reflection of oceanic waters, III. Implication of bi-directionality for the remote-sensing problem, Appl. Optics, 35, 4850–4862, 1996.
Morel, A., Huot, Y., Gentili, B., Werdell, P. J., Hooker, S. B., and Franz, B. A., Examining the consistency of products derived in open ocean (Case 1) waters in the perspective of a multi-sensor approach, Remote Sens. Environ., 111, 69–88, 2007.
Paulson, C. A. and Simpson, J. J.: Irradiance measurements in the upper ocean, J. Phys. Oceanogr, 7, 952–956, 1977.
Preisendorfer, R. W.: Secchi disk science: Visual optics of natural waters, Limnol. Oceanogr., 31, 909–926, 1986.
Sandén, P. and Håkansson, B.: Long-term trends in Secchi depth in the Baltic Sea, Limnol. Oceanogr., 41, 346–351, 1996.

OSD
10, 1833–1893, 2013

Sauberer, F. and Ruttner, F.: Die Strahlungsverhältnisse der Binnengewässer, Akademische Verlagsgesellschaft, Leipzig, 240 pp., 1941.
Secchi, A.: Esperimente per determinare la transparenza del mare, in: Sulmoto ondoso del mare e su le correnti di esso specialmente su quelle littorali, edited by: Cialdi, A., Rome, 258–288, 1866.
Shifrin, K. S.: Physical Optics of Ocean Water, Am. Inst. Phys., New York, 285 pp., 1988.
Sørensen, K. and Aas, E.: Remote sensing of water quality, Proc. SPIE vol. 2258, Ocean Optics XII, edited by: Jaffe, J. S., 332–341, 1994.
Sørensen, K., Aas, E., Faafeng, B., and Lindell, T.: Remote sensing of water quality, NIVA Rep., ISBN 82-577-2262-6, 115 pp., 1993 (in Norwegian).
Sørensen, K., Høkedal, J., Aas, E., Doerffer, R., and Dahl, E.: Early results for validation of MERIS water products in the Skagerrak, in: Proceedings of Envisat Validation Workshop, 9–13 December 2002, Frascati, Italy, ESA SP-531, March 2003, 10 pp., 2003.
Sørensen, K., Aas, E., Høkedal, J., Severinsen, G., Doerffer, R., and Dahl, E.: Validation of MERIS water products in the Skagerrak, in: MAVT Workshop. Proceedings of Envisat Validation Workshop, 20–24 October 2003, Frascati, Italy, ESA CD-ROM, 13 pp., 2004.
Sørensen, K., Aas, E., and Høkedal, J.: Validation of MERIS water products and bio-optical relationships in the Skagerrak, Int. J. Remote Sens., 28, 555–568, 2007.
Takenouti, Y.: On the transparency of sea water, Oceanogr. Mag., Tokyo, 4, 129–135, 1950.
Tyler, J. E.: The Secchi disc, Limnol. Oceanogr., 13, 1–6, 1968.
Walsh, J. W.: Photometry, Dover, New York, 544 pp., 1958.
Wernand, M. R.: On the history of the Secchi disk, J. Eur. Opt. Soc., Rap. Publ., 5, 100135-1-6, 2010.
WMO: Guide to wave analysis and forecasting, 2nd edn., WMO-No. 702, 159 pp., 1998.
Zhang, Y., Pulliainen, J., Koponen, S., and Hallikainen, M., Empirical algorithms for Secchi disk depth using optical and microwave remote sensing data from the Gulf of Finland and the Archipelago Sea, Boreal Environ. Res., 8, 251–261, 2003.
Zibordi, G. and Ferrari, G. M.: Instrument self-shading in underwater optical measurements: experimental data, Appl. Optics, 34, 2750–2754, 1995.

OSD
10, 1833–1893, 2013

Table 1a. Statistical properties of the spectral upward radiance and luminance just beneath the surface at different wavelengths, based on 48 selected stations from the Oslofjord–Skagerrak area.

Wavelength [nm]	412	443	490	510	555	665
	Upward radiance [10^{-2} mW m^{-2} sr^{-1} nm^{-1}]					
Mean value	180	280	420	440	440	82
Stand. dev.	200	320	470	490	490	84
Min. value	12	22	35	37	35	6.2
Max. value	1140	1870	2810	3040	3110	410
	Upward luminance [10^{-2} cd m^{-2} nm^{-1}]					
Mean value	0.18	5.1	59	150	300	2.5
Stand. dev.	0.21	5.9	67	169	330	2.6
Min. value	0.01	0.4	5	13	24	0.2
Max. value	1.16	34.5	400	1040	2120	12.5

OSD
10, 1833–1893, 2013

Table 1b. The same data as Table 1a, but the radiances and luminances are normalized to the value at 555 nm.

Wavelength [nm]	412	443	490	510	555	665
	Upward radiance [%]					
Mean value	44	66	98	102	100	20
Stand. dev.	24	27	27	19		10
Min. value	11	28	55	68		10
Max. value	140	190	210	170		60
	Upward luminance [%]					
Mean value	0.07	1.8	20	51	100	0.9
Stand. dev.	0.04	0.7	6	10		0.5
Min. value	0.02	0.8	12	34		0.5
Max. value	0.21	5.0	43	85		2.7

OSD
10, 1833–1893, 2013

Table 2. Wavelength λ_p of peak value and half-peak bandwidth $\Delta\lambda$ of the eye's photopic sensitivity and the upward spectral luminance L_u; open and with filters.

	Open (white and black disk)	Blue filter	Green filter	Red filter
Eye's sensitivity				
λ_p [nm]	555	460	540	620
$\Delta\lambda$ [nm]	100	48	56	38
L_u				
λ_p [nm]	555	470	540	620
$\Delta\lambda$ [nm]	78	47	55	34

OSD
10, 1833–1893, 2013

Table 3. Mean value and standard deviation of the different quantities and terms of Eqs. (19) and (20) in the Oslofjord and Skagerrak, for the 30 cm white and black disks. Recordings of radiance and irradiance at 32 stations have been applied.

	White	Blue filter	Green filter	Red filter	Black
Z_D [m]	7.8 ± 2.7	4.1 ± 1.4	5.7 ± 2.0	4.2 ± 1.5	2.0 ± 0.7
$(c_{phot} + K_L)_{phot}$ [m^{-1}]	1.09 ± 0.67	1.41 ± 0.99	1.08 ± 0.67	1.48 ± 0.56	1.11 ± 0.68
c_{phot} [m^{-1}]	0.83 ± 0.51	0.97 ± 0.65	0.83 ± 0.52	1.03 ± 0.41	0.84 ± 0.51
$K_{L,phot}$ [m^{-1}]	0.26 ± 0.19	0.44 ± 0.36	0.25 ± 0.18	0.45 ± 0.18	0.27 ± 0.19
ρ_{DL} [%]	29 ± 0	27 ± 1	29 ± 0	30	0
$R_L(0)$ [%]	0.56 ± 0.37	0.47 ± 0.38	0.70 ± 0.47	0.17 ± 0.12	0.56 ± 0.37
$R_L(Z_D)$ [%]	0.83 ± 1.38	0.66 ± 1.33	0.80 ± 1.09	0.28 ± 0.13	0.61 ± 0.51
$\overline{\rho}_{L,air}$ [%]	0.12 ± 0.08	0.20 ± 0.10	0.14 ± 0.09	0.10 ± 0.08	0.12 ± 0.08
$\Re$ [%]	51	51	51	51	51
C_t [%]	0.56 ± 0.02	0.67 ± 0.12	0.56 ± 0.03	0.59 ± 0.10	−0.54 ± 0.01
W [%]	33 ± 23	66 ± 25	49 ± 27	64 ± 25	94 ± 8
$\ln(A_1)$	3.9 ± 0.7	4.1 ± 0.7	3.8 ± 0.6	4.7 ± 0.4	0
$\ln(A_2)$	0.4 ± 0.1	0.7 ± 0.2	0.4 ± 0.1	0.9 ± 0.3	0.4 ± 0.1
$\ln(W)$	−1.3 ± 0.7	−0.5 ± 0.4	−0.9 ± 0.6	−0.5 ± 0.4	−0.1 ± 0.1
$\ln(C_t)$	−5.2 ± 0.0	−5.0 ± 0.2	−5.2 ± 0.1	−5.1 ± 0.1	−5.2 ± 0.0
$\ln(A)$	7.3 ± 0.9	7.9 ± 0.7	7.8 ± 0.8	8.4 ± 0.7	4.7 ± 0.1
$Z_D(c + K_L)_{phot}$	7.0 ± 1.3	4.8 ± 1.2	5.1 ± 0.9	5.5 ± 0.7	1.9 ± 0.3

OSD
10, 1833–1893, 2013

Table 4. Linear relationships on the forms $y = A + Bx$ and $y = B_0 x$ obtained by correlation analysis of Z_D (disk) and Z_B (bowl) observed by the the open eye and with blue, green and red glass filters. Mean values of y/x and y and the standard deviation of y/x are included The size of the disk is 30 cm if not otherwise indicated. r is the correlation coefficient and N is the number of data pairs (y, x).

y	x	r	A [m]	B	B_0	$(y/x)_{\text{mean} \pm \text{sd}}$	y_{mean} [m]	N
$Z_{\text{D, blue}}$	$Z_{\text{D, white}}$	0.89	0.2	0.49	0.52	0.53 ± 0.10	4.0	25
$Z_{\text{D, green}}$	$Z_{\text{D, white}}$	0.96	−0.5	0.79	0.73	0.71 ± 0.09	5.5	25
$Z_{\text{D, red}}$	$Z_{\text{D, white}}$	0.94	0.5	0.48	0.54	0.56 ± 0.08	4.2	25
$Z_{B, \textit{black}}$	$Z_{\text{D, black}}$	0.63	0.8	0.77	1.20	1.29 ± 0.44	2.2	19
$Z_{B, \textit{black}}$	$Z_{\text{D, white}}$	0.11	1.9	0.03	0.23	0.26 ± 0.11	2.2	19
$Z_{\text{D, black}}$	$Z_{\text{D, white}}$	0.54	0.8	0.17	0.26	0.29 ± 0.10	2.2	50
$Z_{\text{D, white, 10}}$	$Z_{\text{D, white,30}}$	0.99	−0.4	0.85	0.81	0.80 ± 0.06	6.9	21
$Z_{\text{D, blue, 10}}$	$Z_{\text{D, blue,30}}$	0.98	−0.1	0.91	0.90	0.88 ± 0.08	3.2	13
$Z_{\text{D, green, 10}}$	$Z_{\text{D, green,30}}$	0.94	1.0	0.96	0.83	0.87 ± 0.12	5.3	13
$Z_{\text{D, red, 10}}$	$Z_{\text{D, red,30}}$	0.95	0.1	0.88	0.90	0.91 ± 0.10	3.9	13
$Z_{\text{D,all, 10}}$	$Z_{\text{D,all,30}}$	0.98	0.4	0.78	0.83	0.86 ± 0.10	5.1	60
$Z_{\text{D, white, shade}}$	$Z_{\text{D, white, sun}}$	0.96	−0.2	0.99	0.97	0.97 ± 0.10	8.3	34
$Z_{\text{D, blue, shade}}$	$Z_{\text{D, blue, sun}}$	0.91	0.5	0.74	0.83	0.87 ± 0.15	4.1	29
$Z_{\text{D, green, shade}}$	$Z_{\text{D, green, sun}}$	0.94	0.1	0.90	0.91	0.91 ± 0.12	5.6	29
$Z_{\text{D, red, shade}}$	$Z_{\text{D, red, sun}}$	0.85	0.4	0.82	0.89	0.91 ± 0.16	4.0	29
$Z_{\text{D, white, 10, tel}}$	$Z_{\text{D, white, 10}}$	0.96	−1.0	1.37	1.22	1.14 ± 0.20	7.2	15
$Z_{\text{D, blue, 10, tel}}$	$Z_{\text{D, blue, 10}}$	0.93	−0.1	1.18	1.15	1.14 ± 0.18	3.3	11
$Z_{\text{D, green, 10, tel}}$	$Z_{\text{D, green, 10}}$	0.96	−0.7	1.27	1.15	1.09 ± 0.15	5.2	11
$Z_{\text{D, red, 10, tel}}$	$Z_{\text{D, red, 10}}$	0.92	0.1	1.14	1.15	1.16 ± 0.18	4.2	11
$Z_{\text{D,all, 10, tel}}$	$Z_{\text{D,all, 10}}$	0.96	−0.5	1.28	1.19	1.14 ± 0.18	5.2	48

OSD
10, 1833–1893, 2013

Table 5. Linear relationships on the forms $y = A + Bx$ and $y = B_0 x$ obtained by correlation analysis of attenuation coefficients of spectrally integrated luminance for the open eye and with blue, green and red glass filters and coefficients of monochromatic radiance at 470, 540, 555 and 620 nm, and mean values of y/x and y. The attenuation coefficients are averages over the depth range 0–Z_D. r is the correlation coefficient. The error ε is the root-mean-square of the deviations ($y - A - Bx$), and ε_0 is the rms of ($y - B_0 x$). The analysis is based on 32 stations.

y	x	r	A [m^{-1}]	B	B_0	$(y/x)_{mean \pm sd}$	y_{mean} [m^{-1}]	ε [m^{-1}]	ε_0 [m^{-1}]
$c_{phot,\,disk}$	c_{555}	1.00	0.02	0.99	1.01	1.02 ± 0.01	0.83	0.01	0.02
c_{phot}	c_{555}	1.00	0.01	1.00	1.01	1.02 ± 0.01	0.83	0.01	0.01
$K_{L,\,phot}$	$K_{L,\,555}$	1.00	0.00	1.12	1.12	1.11 ± 0.05	0.26	0.01	0.01
$(c + K_L)_{phot}$	$(c + K_L)_{555}$	1.00	0.00	1.03	1.03	1.03 ± 0.01	1.09	0.01	0.01
$c_{phot,\,blue}$	c_{470}	1.00	0.06	0.90	0.95	0.98 ± 0.04	0.97	0.04	0.05
$c_{phot,\,green}$	c_{540}	1.00	0.02	0.97	0.98	1.00 ± 0.01	0.83	0.01	0.02
$c_{phot,\,red}$	c_{620}	1.00	0.18	0.91	1.06	1.12 ± 0.07	1.03	0.03	0.08
$K_{L,\,phot,\,blue}$	$K_{L,\,470}$	0.99	0.05	0.95	1.01	1.10 ± 0.05	0.44	0.04	0.05
$K_{L,\,phot,\,green}$	$K_{L,\,540}$	1.00	0.01	0.96	0.98	1.00 ± 0.01	0.25	0.00	0.01
$K_{L,\,phot,\,red}$	$K_{L,\,620}$	0.99	0.09	1.05	1.21	1.27 ± 0.08	0.45	0.02	0.04
$(c + K_L)_{phot,\,blue}$	$(c + K_L)_{470}$	1.00	0.11	0.92	0.97	1.02 ± 0.04	1.41	0.07	0.09
$(c + K_L)_{phot,\,green}$	$(c + K_L)_{540}$	1.00	0.03	0.96	0.98	1.00 ± 0.01	1.08	0.01	0.02
$(c + K_L)_{phot,\,red}$	$(c + K_L)_{620}$	1.00	0.25	0.94	1.10	1.16 ± 0.07	1.48	0.04	0.11

OSD
10, 1833–1893, 2013

Table 6. Relationships on the forms $y = A + Bx$ and $y = B_0 x$, where A, B and B_0 are coefficients from the correlation analysis between y and $x = 1/Z_{D,\,white}$. The error ε is the root-mean-square of the deviations ($y - A - Bx$), and ε_0 is the rms of ($y - B_0 x$). r is the correlation coefficient and N is the number of stations.

y	r	A [m^{-1}]	B	B_0	$(y/x)_{mean \pm sd}$	y_{mean} [m^{-1}]	ε [m^{-1}]	ε_0 [m^{-1}]	N
c_{412}	0.86	−0.24	10.6	9.6	8.8 ± 2.3	1.67	0.58	0.60	79
c_{443}	0.91	−0.23	9.0	8.0	7.2 ± 1.7	1.38	0.37	0.39	79
c_{490}	0.94	−0.22	7.6	6.6	6.0 ± 1.2	1.14	0.22	0.28	79
c_{510}	0.95	−0.21	7.2	6.4	5.7 ± 1.1	1.10	0.20	0.26	79
c_{555}	0.95	−0.17	6.6	5.9	5.4 ± 1.0	1.01	0.18	0.20	79
c_{620}	0.95	0.03	6.1	6.3	6.3 ± 0.9	1.14	0.18	0.18	79
c_{665}	0.93	0.18	5.8	6.5	6.9 ± 1.1	1.21	0.19	0.21	79
$K_{L,412}$	0.66	0.01	4.6	4.6	4.5 ± 1.8	0.91	0.57	0.57	53
$K_{L,443}$	0.64	−0.05	4.2	4.0	3.7 ± 2.0	0.78	0.55	0.55	53
$K_{L,490}$	0.72	−0.02	2.4	2.3	2.2 ± 0.9	0.45	0.25	0.25	53
$K_{L,510}$	0.72	0.00	2.0	2.0	1.9 ± 0.7	0.39	0.21	0.21	53
$K_{L,555}$	0.72	0.05	1.3	1.5	1.6 ± 0.5	0.31	0.14	0.14	53
$K_{L,620}$	0.77	0.15	1.5	2.1	2.4 ± 0.7	0.45	0.14	0.15	53
$K_{L,665}$	0.78	0.22	1.7	2.5	3.0 ± 0.8	0.55	0.15	0.18	53
$K_{d,412}$	0.59	−0.02	5.9	5.8	5.4 ± 3.3	1.14	0.89	0.89	53
$K_{d,443}$	0.64	−0.05	4.2	4.0	3.7 ± 2.0	0.78	0.55	0.55	53
$K_{d,490}$	0.70	−0.03	2.5	2.4	2.2 ± 1.0	0.46	0.28	0.28	53
$K_{d,510}$	0.71	−0.02	2.1	2.0	1.9 ± 0.8	0.40	0.22	0.22	53
$K_{d,555}$	0.74	0.02	1.4	1.5	1.5 ± 0.5	0.30	0.14	0.14	53
$K_{d,620}$	0.82	0.25	1.2	2.2	2.8 ± 0.8	0.49	0.09	0.15	53
$K_{d,665}$	0.86	0.41	1.1	2.7	3.7 ± 1.2	0.62	0.07	0.21	53
$K_{u,412}$	0.43	0.18	6.5	7.2	7.0 ± 6.5	1.42	1.43	1.43	51
$K_{u,443}$	0.52	0.05	5.2	5.4	5.1 ± 3.5	1.05	0.92	0.92	51
$K_{u,490}$	0.67	−0.03	3.1	3.0	2.8 ± 1.4	0.58	0.38	0.38	53
$K_{u,510}$	0.68	0.00	2.5	2.5	2.4 ± 1.1	0.50	0.30	0.30	53
$K_{u,555}$	0.64	0.06	1.6	1.9	2.0 ± 0.8	0.38	0.21	0.22	53
$K_{u,620}$	0.71	0.20	1.9	2.7	3.1 ± 1.1	0.58	0.21	0.23	53
$K_{u,665}$	0.72	0.30	2.1	3.3	3.9 ± 1.3	0.71	0.22	0.26	53

OSD
10, 1833–1893, 2013

Table 7. Relationships on the forms $y = A + Bx$ and $y = B_0 x$ obtained by correlation analysis of attenuation coefficients of monochromatic radiance and irradiance and Secchi disk depths observed with the open eye and with blue, green and red glass filters. The attenuation coefficients are averages over the depth range $0–Z_D$, and r is the correlation coefficient. The error ε is the root-mean-square of the deviations ($y – A – Bx$), and ε_0 is the rms of ($y – B_0 x$). The analysis is based on 25 stations.

y	x	r	A [m^{-1}]	B	B_0	$(y/x)_{mean \pm sd}$	y_{mean} [m^{-1}]	ε [m^{-1}]	ε_0 [m^{-1}]
c_{470}	$1/Z_{D,\,blue}$	0.84	−0.23	4.3	3.7	3.4 ± 1.1	1.1	0.42	0.43
c_{470}	$1/Z_{D,\,white}$	0.94	−0.34	9.0	7.3	6.4 ± 1.6	1.1	0.26	0.30
c_{540}	$1/Z_{D,\,green}$	0.94	−0.12	4.5	4.1	3.9 ± 0.9	0.91	0.19	0.20
c_{540}	$1/Z_{D,\,white}$	0.96	−0.18	6.9	5.9	5.5 ± 1.1	0.91	0.15	0.17
c_{620}	$1/Z_{D,\,red}$	0.89	0.24	2.6	3.3	3.6 ± 0.7	1.0	0.22	0.25
c_{620}	$1/Z_{D,\,white}$	0.97	0.09	5.7	6.2	6.4 ± 0.9	1.0	0.12	0.13
$K_{L,\,470}$	$1/Z_{D,\,blue}$	0.74	−0.17	2.0	1.6	1.4 ± 0.7	0.45	0.28	0.29
$K_{L,\,470}$	$1/Z_{D,\,white}$	0.80	−0.20	4.1	3.1	2.6 ± 1.2	0.45	0.25	0.26
$K_{L,\,540}$	$1/Z_{D,\,green}$	0.79	−0.04	1.3	1.2	1.2 ± 0.4	0.27	0.13	0.13
$K_{L,\,540}$	$1/Z_{D,\,white}$	0.80	−0.06	2.0	1.7	1.6 ± 0.6	0.27	0.12	0.13
$K_{L,\,620}$	$1/Z_{D,\,red}$	0.80	0.11	0.9	1.2	1.4 ± 0.4	0.38	0.11	0.13
$K_{L,\,620}$	$1/Z_{D,\,white}$	0.83	0.07	1.9	2.3	2.5 ± 0.6	0.38	0.10	0.11
$K_{d,\,470}$	$1/Z_{D,\,blue}$	0.73	−0.17	2.0	1.6	1.4 ± 0.7	0.44	0.29	0.29
$K_{d,\,470}$	$1/Z_{D,\,white}$	0.82	−0.21	4.1	3.0	2.6 ± 1.2	0.44	0.24	0.26
$K_{d,\,540}$	$1/Z_{D,\,green}$	0.80	−0.05	1.3	1.2	1.1 ± 0.4	0.26	0.12	0.12
$K_{d,\,540}$	$1/Z_{D,\,white}$	0.81	−0.06	2.0	1.7	1.6 ± 0.5	0.26	0.12	0.12
$K_{d,\,620}$	$1/Z_{D,\,red}$	0.80	0.26	0.62	1.3	1.7 ± 0.4	0.44	0.07	0.15
$K_{d,\,620}$	$1/Z_{D,\,white}$	0.83	0.23	1.3	2.4	3.1 ± 0.8	0.44	0.07	0.13
$K_{u,\,470}$	$1/Z_{D,\,blue}$	0.72	−0.34	3.1	2.2	1.8 ± 1.0	0.60	0.44	0.47
$K_{u,\,470}$	$1/Z_{D,\,white}$	0.78	−0.38	6.2	4.3	3.4 ± 2.0	0.60	0.39	0.43
$K_{u,\,540}$	$1/Z_{D,\,green}$	0.80	−0.06	1.6	1.4	1.4 ± 0.5	0.31	0.15	0.15
$K_{u,\,540}$	$1/Z_{D,\,white}$	0.80	−0.07	2.4	2.0	1.9 ± 0.7	0.31	0.15	0.15
$K_{u,\,620}$	$1/Z_{D,\,red}$	0.77	0.17	1.0	1.5	1.7 ± 0.5	0.47	0.14	0.16
$K_{u,\,620}$	$1/Z_{D,\,white}$	0.82	0.12	2.2	2.8	3.1 ± 1.0	0.47	0.13	0.14

OSD
10, 1833–1893, 2013

Table 8. Linear relationships on the forms $y = A + Bx$ and $y = B_0 x$, obtained by correlation analysis of the vertical attenuation coefficient K_q of downward quanta irradiance, the depths $Z_q(p\%)$ where the quanta irradiance is reduced to p percent of the surface value, and the Secchi disk depth $Z_{D,\,white}$. The error ε is the root-mean-square of the deviations $(y - A - Bx)$, ε_0 is the rms of $(y - B_0 x)$, and r is the correlation coefficient. The analysis is based on 205 stations.

y	x	r	A [m^{-1}]	B	B_0	$(y/x)_{mean \pm sd}$	y_{mean} [m^{-1}]	ε [m^{-1}]	ε_0 [m^{-1}]
K_q	$1/Z_{D,\,white}$	0.89	0.13	1.8	2.3	2.5 ± 0.5	0.54	0.10	0.11
y	x	r	A [m]	B	B_0	$(y/x)_{mean \pm sd}$	y_{mean} [m]	ε [m]	ε_0 [m]
$Z_q(30\,\%)$	$Z_{D,\,white}$	0.72	1.0	0.22	0.36	0.44 ± 0.16	2.3	0.6	0.7
$Z_q(10\,\%)$	$Z_{D,\,white}$	0.78	2.1	0.47	0.77	0.92 ± 0.30	4.9	1.0	1.4
$Z_q(3\,\%)$	$Z_{D,\,white}$	0.79	3.5	0.79	1.3	1.5 ± 0.5	8.1	1.7	2.2
$Z_q(1\,\%)$	$Z_{D,\,white}$	0.74	5.0	1.1	1.8	2.2 ± 0.7	11.5	2.8	3.5
$Z_q(30\,\%)$	$Z_q(1\,\%)$	0.80	0.4	0.16	0.20	0.20 ± 0.04	2.3	0.5	0.5
$Z_q(10\,\%)$	$Z_q(1\,\%)$	0.91	0.7	0.36	0.41	0.43 ± 0.06	4.9	0.7	0.7
$Z_q(3\,\%)$	$Z_q(1\,\%)$	0.97	0.6	0.65	0.69	0.70 ± 0.05	8.1	0.6	0.6

OSD
10, 1833–1893, 2013

Table 9. Relationships on the forms $y = A + Bx$ and $y = B_0 x$ obtained by correlation analysis of chlorophyll *a* (Chl), total suspended material (TSM) and inverse Secchi disk depths ($1/Z_D$) observed with the open eye and with blue, green and red glass filters. The concentrations of Chl and TSM are averages over the depth range 0–Z_D, and r is the correlation coefficient. The error ε is the root-mean-square of the deviations ($y - A - Bx$), and ε_0 is the rms of ($y - B_0 x$). The analysis is based on 19 stations.

y	x	r	A [mg m^{-3}]	B [mg m^{-2}]	B_0 [mg m^{-2}]	$(y/x)_{\text{mean}\pm\text{sd}}$ [mg m^{-2}]	y_{mean} [mg m^{-3}]	ε [mg m^{-3}]	ε_0 [mg m^{-3}]
Chl	$1/Z_{\text{D, white}}$	0.64	0.71	4.9	8.3	10.0 ± 3.8	1.5	0.5	0.6
Chl	$1/Z_{\text{D, blue}}$	0.72	0.62	3.0	4.6	5.5 ± 2.0	1.5	0.4	0.5
Chl	$1/Z_{\text{D, green}}$	0.65	0.74	3.3	5.7	7.3 ± 3.2	1.5	0.5	0.6
Chl	$1/Z_{\text{D, red}}$	0.54	0.94	1.9	4.2	5.6 ± 2.3	1.5	0.5	0.7
y	x	r	A [g m^{-3}]	B [g m^{-2}]	B_0 [g m^{-2}]	$(y/x)_{\text{mean}\pm\text{sd}}$ [g m^{-2}]	y_{mean} [g m^{-3}]	ε [g m^{-3}]	ε_0 [g m^{-3}]
TSM	$1/Z_{\text{D, white}}$	0.66	0.22	6.0	7.0	7.7 ± 3.9	1.2	0.6	0.6
TSM	$1/Z_{\text{D, blue}}$	0.46	0.54	2.2	3.6	4.4 ± 2.3	1.2	0.7	0.7
TSM	$1/Z_{\text{D, green}}$	0.58	0.40	3.4	4.7	5.7 ± 3.2	1.2	0.6	0.6
TSM	$1/Z_{\text{D, red}}$	0.65	0.39	2.7	3.6	4.4 ± 2.3	1.2	0.6	0.6

OSD
10, 1833–1893, 2013

Table 10. Nomenclature.

Symbol	Description	Introduced
A	dimensionless function	Eq. (20)
A	constant of correlation analysis	Sect. 5
A_1	dimensionless function	Eq. (21)
A_2	dimensionless function	Eq. (21)
a_{bp}	absorption coefficient of bleached particles	Sect. 3
a_y	absorption coefficient of yellow substance	Sect. 3
B	constant of correlation analysis	Sect. 5
B_0	constant of correlation analysis	Sect. 5
b_p	scattering coefficient of particles	Sect. 3
C	visual contrast between Secchi disk and background	Eq. (1)
C_{air}	contrast of the Secchi disk observed in air	Eq. (13)
Chl	concentration of chlorophyll *a*	Sect. 3
C_t	visual threshold contrast	Eq. (1)
c	beam attenuation coefficient	Eq. (2)
c_{phot}	beam attenuation coefficient for nadir luminance	Sect. 4.1
D	diameter of the Secchi disk	Eq. (14)
E_{air}	downward illuminance or irradiance in air	Eq. (17)
E_d	downward illuminance or irradiance in the sea	Eq. (6)
E_u	upward illuminance or irradiance in the sea	Sect. 3
H	height of the observer's eye above the surface of the sea	Eq. (22)
j	angle of refraction in water	Eq. (22)
K_d	average vertical attenuation coefficient of downward irradiance	Sect. 6.1
K_L	average vertical attenuation coefficient of $L(z)$	Eq. (9)
$K_{L,\,phot}$	average vertical attenuation coefficient of luminance from nadir	Sect. 4.1
K_q	average vertical attenuation coefficient of quanta irradiance (PAR)	Eq. (24)
K_u	average vertical attenuation coefficient of upward irradiance	Sect. 6.1
k	$787\,m\,s^{-1}$	Eq. (14)
L	nadir radiance and luminance from the background in the sea	Eq. (1)
L_D	nadir radiance and luminance from the Secchi disk	Eq. (1)

OSD
10, 1833–1893, 2013

Table 10. Continued.

L_r	radiance from sun and sky reflected at the surface	Eq. (12)
L_w	water-leaving radiance	Eq. (12)
L_*	path function along path outside the disk	Eq. (3)
L_{*D}	path function along path from disk to observer	Eq. (2)
n	index of refraction for water	Eq. (12)
Q	radiance/irradiance ratio	Sect. 3
R_L	sub-surface radiance reflectance of the sea	Eq. (7)
r	correlation coefficient	Table 4
$\Re$	radiance-irradiance ratio	Eq. (18)
T_D	transmittance of quanta irradiance between the surface and the Secchi depth	Eq. (24)
TSM	concentration of total suspended material	Sect. 3
Turb	turbidity	Sect. 6.3
U	wind speed	Eq. (14)
W	contrast transmittance at the water–air interface	Eq. (14)
x	independent variable	Sect. 5
y	dependent variable	Sect. 5
Z_D	Secchi depth	Eq. (5)
$Z_q(p\%)$	depth where the quanta irradiance is reduced to p% of the surface value	Sect. 6.2
z	vertical coordinate, positive downwards, zero at surface	Eq. (2)
α	apparent angle from the observer's eye across the Secchi disk	Eq. (22)
ε	root-mean-squares error	Sect. 5
ε_0	root-mean-squares error	Sect. 5
λ	wavelength	Sect. 3
ρ_{DL}	luminance or radiance reflectance of the Secchi disk	Eq. (6)
$\overline{\rho}_{L,\,air}$	Fresnel-reflected luminance or radiance towards the zenith	Eq. (17)
τ	luminance or radiance transmittance for a ray of normal incidence at the water–air interface	Eq. (12)

OSD
10, 1833–1893, 2013

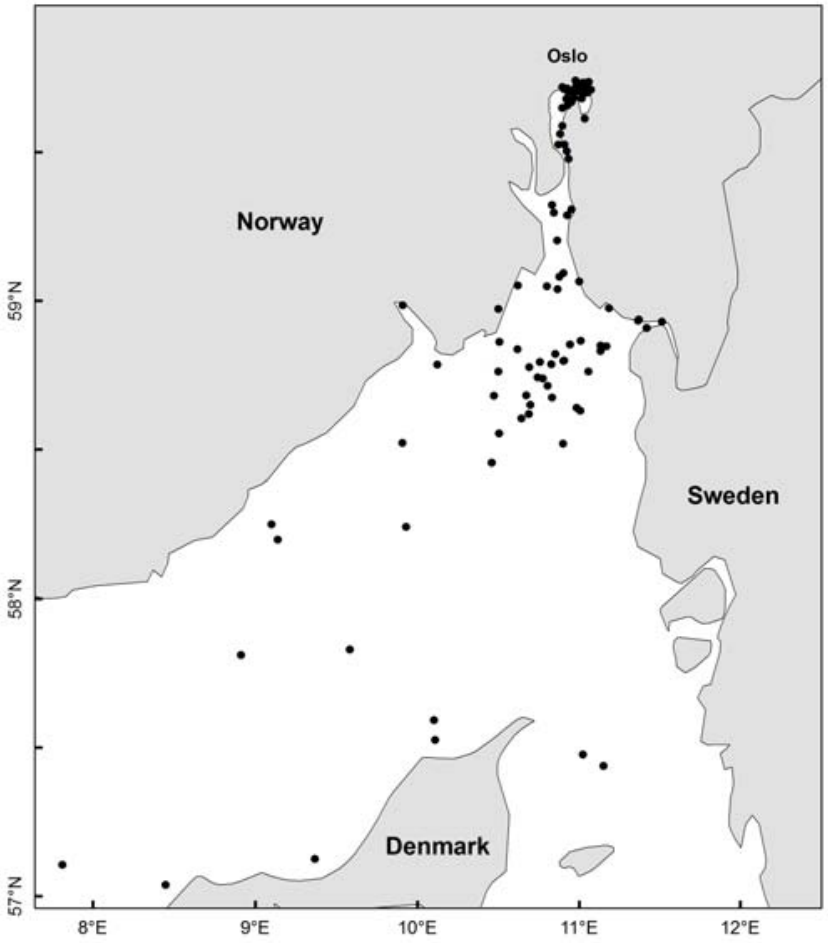

Fig. 1. Locations of the stations.

OSD
10, 1833–1893, 2013

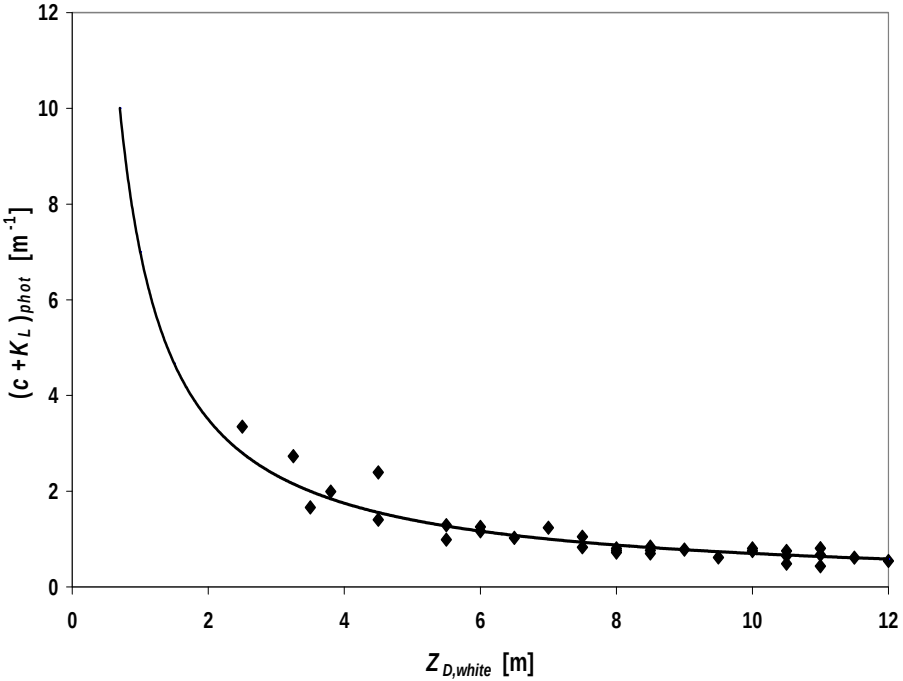

Fig. 2. $(c + K_L)_{\text{phot}}$ as a function of $Z_{\text{D, white}}$. The line is the function $(c + K_L)_{\text{phot}} = 7.0/Z_{\text{D, white}}$.

OSD
10, 1833–1893, 2013

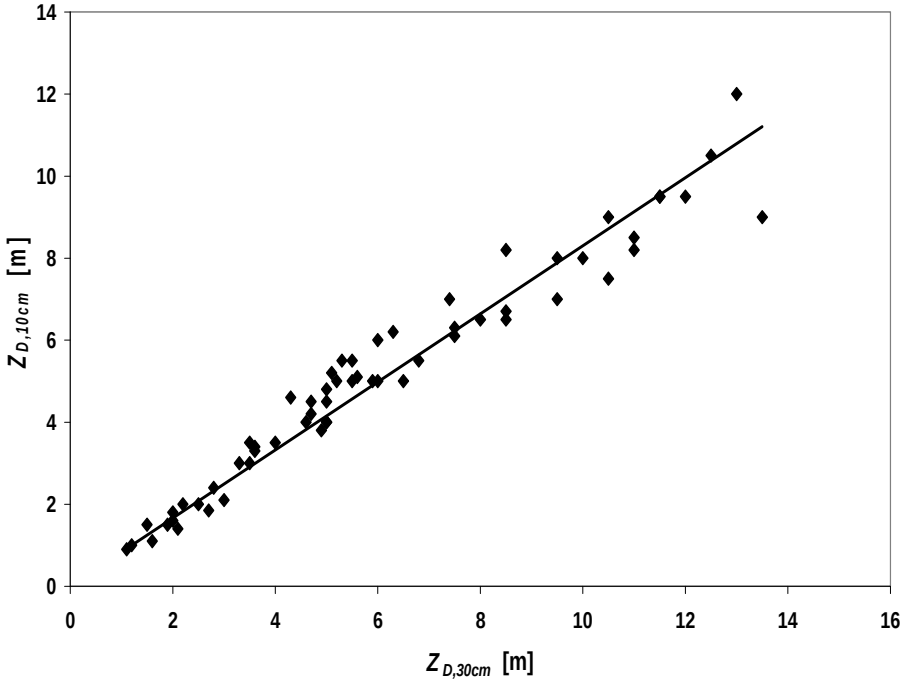

Fig. 3. All naked eye and colour filter observations of Z_D with a 10 cm disk as a function of the observations with a 30 cm disk. The best-fit line through the origin is the function $Z_{D,\,10\,cm} = 0.83 Z_{D,\,30\,cm}$.

OSD
10, 1833–1893, 2013

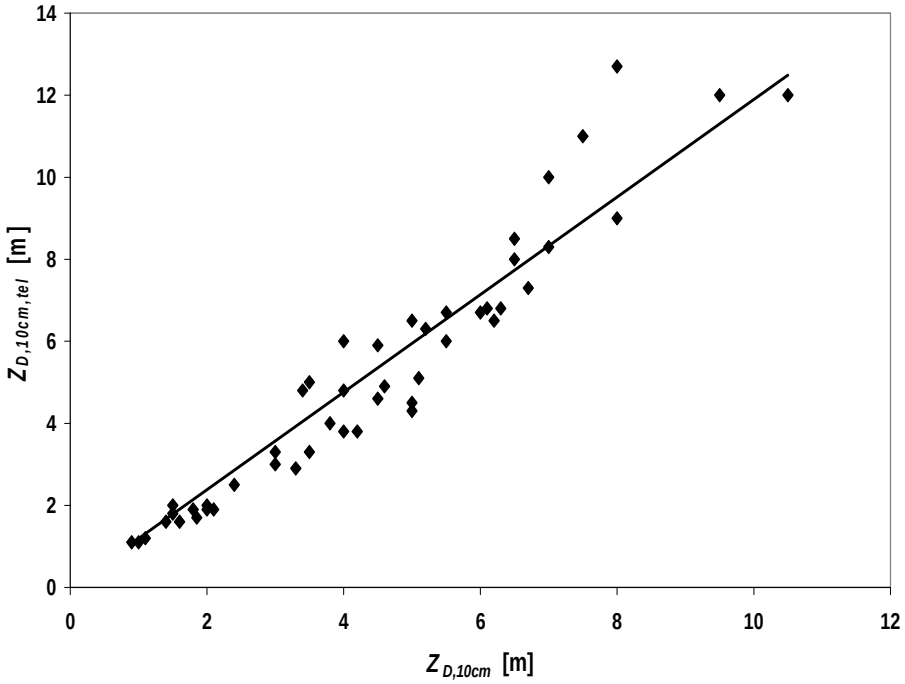

Fig. 4. All naked eye and colour filter observations of $Z_{\mathrm{D,\,10\,cm,\,tel}}$ with a telescope as a function of $Z_{\mathrm{D,\,10\,cm}}$ without telescope. The best-fit line through the origin is the function $Z_{\mathrm{D,\,10\,cm,\,tel}} = 1.19 Z_{\mathrm{D,\,10\,cm}}$.

OSD
10, 1833–1893, 2013

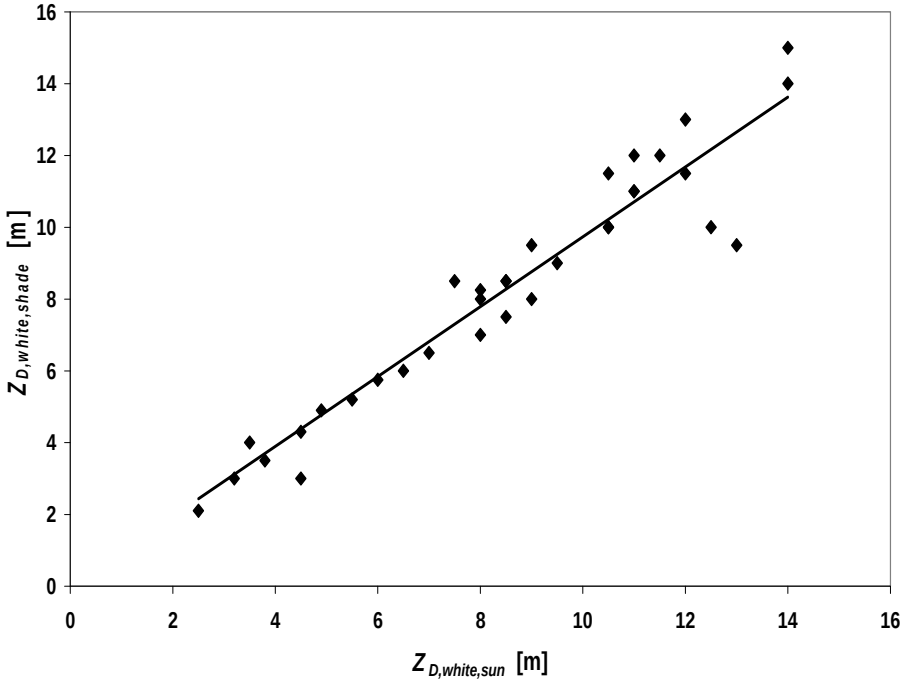

Fig. 5. $Z_{D,\,white}$ observed on the shaded and sunlit sides of the ship. The best-fit line through the origin is the function $Z_{D,\,white,\,shade} = 0.97 Z_{D,\,white,\,sun}$.

OSD
10, 1833–1893, 2013

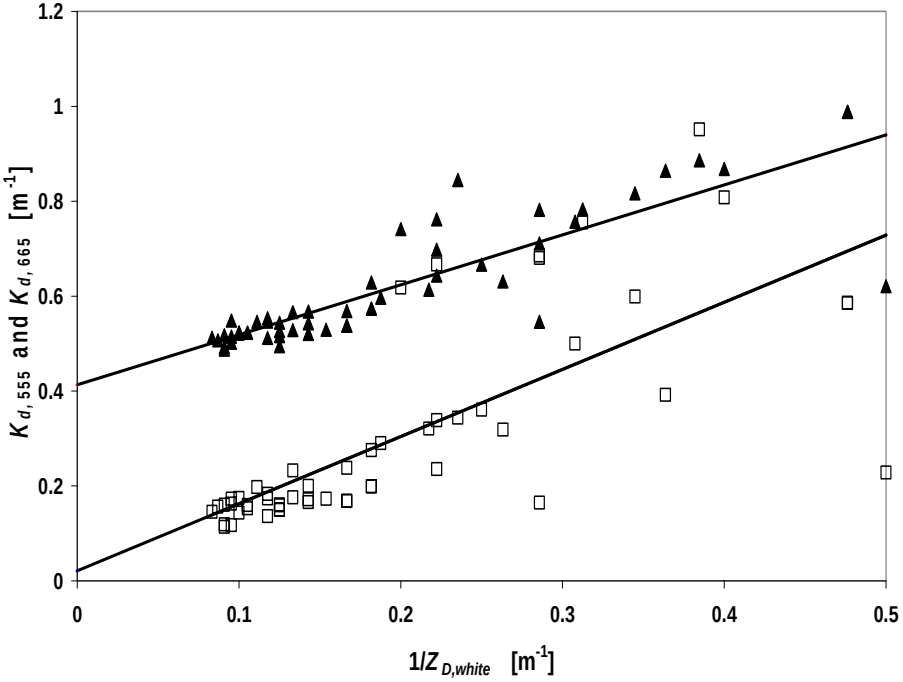

Fig. 6. K_d at 555 nm (open squares) and 665 nm (triangles) as a function of $1/Z_{D,\,white}$. The upper best-fit line is the function $K_{d,\,665} = [0.41\,m^{-1}] + 1.1/Z_{D,\,white}$ and the lower line is $K_{d,\,555} = [0.02\,m^{-1}] + 1.4/Z_{D,\,white}$.

OSD
10, 1833–1893, 2013

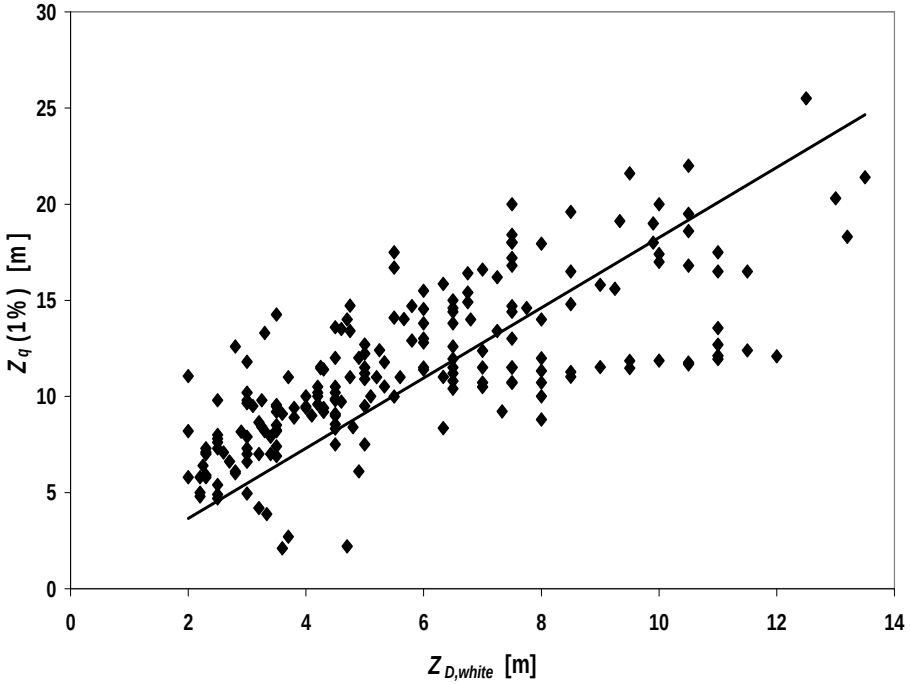

Fig. 7. The depth of the euphotic zone, $Z_q(1\,\%)$, as a function of the Secchi depth $Z_{D,\,white}$. The best fit line through the origin is $Z_q(1\,\%) = 1.8 Z_{D,\,white}$.

OSD
10, 1833–1893, 2013

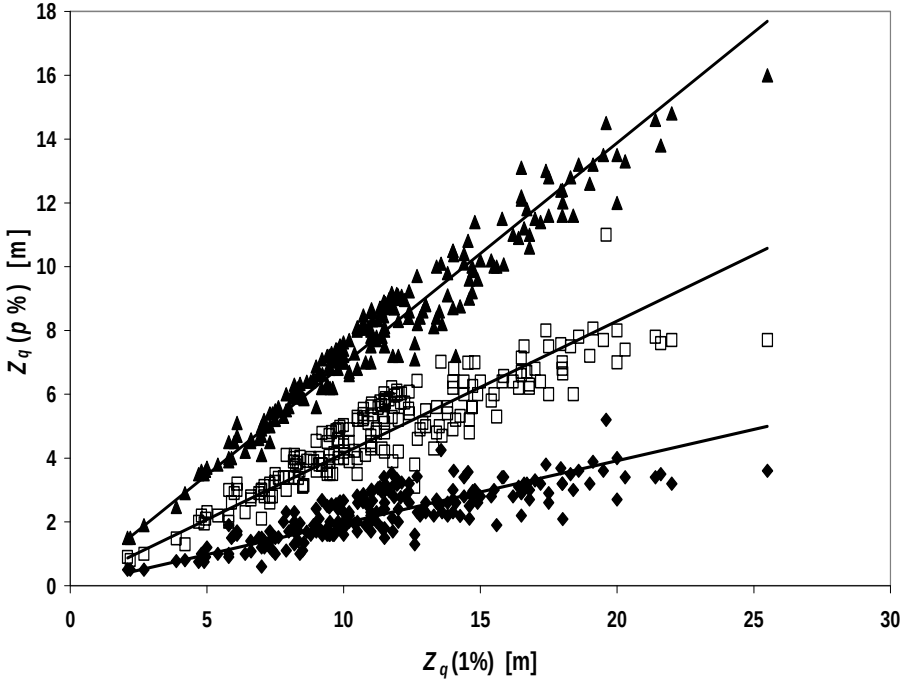

Fig. 8. $Z_q(p\%)$ as a function of $Z_q(1\,\%)$ for $p = 3$ (triangles), $p = 10$ (open squares), $p = 30$ (diamonds). The best-fit lines through the origin are $Z_q(3\,\%) = 0.69 Z_q(1\,\%)$, $Z_q(10\,\%) = 0.41 Z_q(1\,\%)$. and $Z_q(30\,\%) = 0.20 Z_q(1\,\%)$.

OSD
10, 1833–1893, 2013